Available online at www.sciencedirect.com
SCIENCE DIRECT
Tectonophysics 420 (2006) 431–454
TECTONOPHYSICS
www.elsevier.com/locate/tecto

Stratigraphic evidence for millennial-scale temporal clustering of earthquakes on a continental-interior fault: Holocene Mississippi River floodplain deposits, New Madrid seismic zone, USA

John Holbrook [a,*], Whitney J. Autin [b,1], Tammy M. Rittenour [e,2], Stephen Marshak [d,3], Ronald J. Goble [c,4]

[a] Department of Earth and Environmental Sciences, University of Texas at Arlington, Arlington, Texas 79019, United States
[b] Department of the Earth Sciences, SUNY College at Brockport, Brockport, New York 14420, United States
[c] Department of Geosciences, University of Nebraska, Lincoln, Nebraska 68588, United States
[d] Department of Geology, University of Illinois, Urbana, Illinois 61801, United States
[e] Department of Geology, Utah State University, Logan, UT 84322, United States

Received 1 August 2005; received in revised form 31 March 2006; accepted 4 April 2006

Abstract

The earthquake cycles that characterize continental-interior areas that are far from active plate boundaries have proven highly cryptic and difficult to resolve. We used a novel paleoseismic proxy to address this issue. Namely, we reconstructed Holocene Mississippi River channels from maps of floodplain strata in order to identify channel perturbations reflective of major displacement events on the high-hazard and mid-plate Reelfoot thrust fault, New Madrid seismic zone, U.S.A. Only three discrete slip events are currently documented for the Reelfoot fault (~AD 900, ~AD 1450, and AD 1812). This study extends this record and, thus, illustrates the utility of stratigraphic proxies as paleoseismic tools. We concurrently offer here some of the first quantified response times for tectonically induced channel pattern changes in large alluvial rivers.

We identified at least two cycles of pervasive meandering that were interrupted by channel-straightening responses occurring upstream of the Reelfoot fault scarp. These straightening responses initiated at 2244 BC+/−269 to 1620 BC+/−220 and ~ AD 900, respectively, and each records initiation of a period of Reelfoot fault slip after millennia of relative tectonic quiescence. The second (or New Madrid) straightening response was triggered by the previously known ~AD 900 fault slip event, and this initial low sinuosity has been protracted until the modern day by the latter ~AD 1450 and AD 1812 events. The first (or Bondurant) straightening response began a period of several hundred to ~1400 years of low river sinuosity which evidences a similar period of multiple recurrent displacement events on the Reelfoot fault. These Bondurant events predate the existing paleoseismic record for the Reelfoot fault.

These data offer initial evidence that slip events on the Reelfoot fault were temporally clustered on millennial scales and, thus, offers the first direct evidence for millennial-scale clustering of earthquakes on a continental-interior fault. This carries additional

* Corresponding author. Tel.: +1 817 272 1201.
E-mail addresses: holbrook@uta.edu (J. Holbrook), dirtguy@esc.brockport.edu (W.J. Autin), tammyr@cc.usu.edu (T.M. Rittenour), smarshak@uiuc.edu (S. Marshak), rgoble@unlnotes.unl.edu (R.J. Goble).
[1] Tel.: +1 585 395 5738.
[2] Tel.: +1 435 797 7097.
[3] Tel.: +1 217 244 4996.
[4] Tel.: +1 402 472 4917.

0040-1951/$ - see front matter
doi:10.1016/j.tecto.2006.04.002

ramifications. Namely, faults that have been quiescent and non-hazardous for millennia could re-enter an enduring period of recurrent hazardous earthquakes with little warning. Likewise, the Reelfoot fault also reveals evidence of temporal clustering of earthquakes on short-term cycles (months), as well as evidence for longer-term reactivation cycles (10^4–10^6 years). This introduces the possibility that temporal clustering could be hierarchical on some continental-interior faults.

Keywords: Paleoseismology; Mississippi River; New Madrid seismic zone; Intraplate tectonics; Temporal clustering; Fault; Stratigraphic proxy; Fluvial

1. Introduction

The earthquake cycle for seismically active fault systems in the weakly compressive and slowly deforming stress provinces that typify mid-continent plate interiors (Zoback and Zoback, 1980; Zoback et al., 1989; Clark and Leonard, 2003; Zoback and Mooney, 2003) has proven challenging to constrain with conventional tools, and is thus poorly understood (Kenner and Segall, 2000; Newman et al., 2001; Chery et al., 2001; Crone et al., 2003; Schulte and Mooney, 2003). Accordingly, the potential role of temporal clustering in co-seismic fault-slip trends within these systems is uncertain. Seismic and near-historic records are helpful in constraining short-term patterns and reveal that temporal clustering of multiple large earthquakes over periods of days to years in such regions is common (Johnston and Schweig, 1996; Spicak, 2000; Mittag, 2003) and potentially the norm (Johnston and Schweig, 1996). The longer-term mid-continent earthquake cycle is more cryptic. Some have suspected that comparable millennial-scale clustering is also common place in continental interiors, based on analogy with structurally similar, yet more active, plate-margin-associated systems where such clustering is well recorded (Peltzer et al., 2001; Chery et al., 2001). Still others have argued for even longer clustering cycles of 10^4–10^6 years, based on direct geologic study of mid-continent structures (Van Arsdale, 2000; Crone et al., 2003).

Here we apply a novel paleoseismic proxy to significantly extend the current slip record on the mid-continent and high-hazard Reelfoot fault in order to evaluate longer-term trends for historically co-seismic slip events. Particularly, we reconstruct channel and floodplain history of the Mississippi River from Holocene strata transecting the active Reelfoot fault, and then assess these reconstructions for evidence of rapid river response to abrupt fault slip. Here we provide an initial case for millennial-scale temporal clustering of large earthquakes on this example mid-continent fault and assess the implications of this evidence for seismic hazard assessment and fault displacement trends in mid-continent regions in general.

2. The Reelfoot fault

The Reelfoot fault is located within the upper Mississippi Embayment of the U.S. Mid-continent region, and exists as a northwest-trending thrust fault linking two northeast-oriented strike-slip faults (Russ, 1982; Odum et al., 1998; Purser and Van Arsdale, 1998) (Fig. 1). The Reelfoot fault and these contiguous strike-slip faults together comprise the high-seismicity New Madrid fault system, currently the main focus of seismic hazard assessment in the U.S. Mid-continent (Cramer et al., 2001; Newman et al., 2001). This fault system is well known for a temporal cluster of at least three large (each as high as Moment Magnitude, $M_o > 7.5$; Johnston and Schweig, 1996; Bakun and Hopper, 2004) intraplate earthquakes during the winter of 1811–12, at least one of which (the last) originated from the Reelfoot fault (Johnston and Schweig, 1996; Odum et al., 1998; Hough et al., 2000; Mueller and Pujol, 2001; Bakun and Hopper, 2004). Dip slip on the Reelfoot blind thrust has produced a hanging-wall anticline (Lake County uplift), with up to 11 m of surficial relief (Russ, 1982; Purser and Van Arsdale, 1998). The Lake County uplift is bound on the northeast by a fault-propagation monocline, which warps surficial strata by up to 9 m and is expressed topographically as the Reelfoot scarp (Russ, 1982; Purser and Van Arsdale, 1998; Mueller et al., 1999; Champion et al., 2001) (Fig. 1). Trenching across the Reelfoot scarp reveals that this monocline originated from three discrete fault displacement events (AD 900 ± 100, AD 1450 ± 150, and AD 1812) (Russ, 1982; Kelson et al., 1996; Guccione et al., 2002). Liquefaction studies show these displacements coincide with the three largest paleoseismic events confirmed regionally and are, thus, co-seismic (Tuttle et al., 1999, 2002). Further, compound liquefaction features suggest the older AD 900 and AD 1450 seismic events are also temporally clustered in 1811–12 fashion (Tuttle et al., 2002). Though liquefaction-based evidence exists for an earlier and likely non-clustered seismic event at AD 300 somewhere within the New Madrid seismic zone, no surficial deformation is found on the Reelfoot scarp for this time and no association of AD 300 seismicity with Reelfoot fault slip is supported (Guccione, 2005).

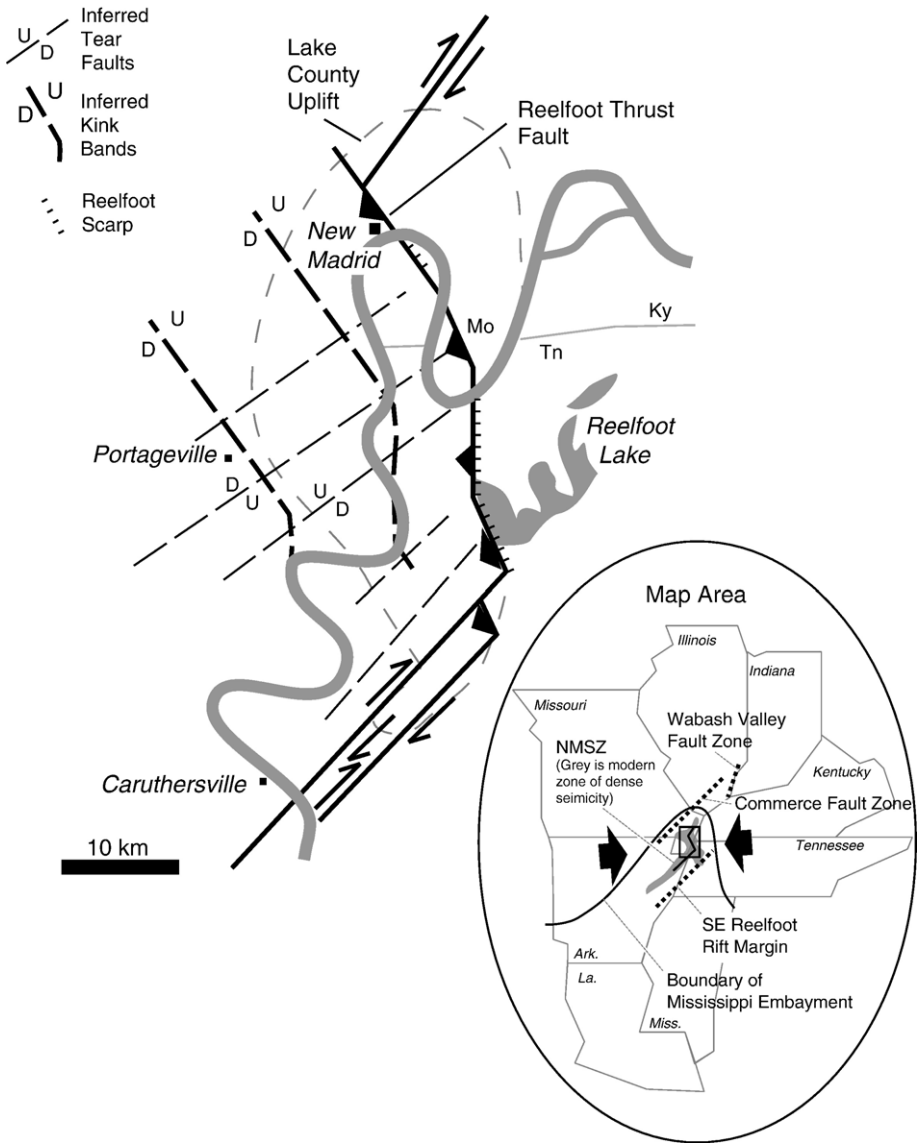

Fig. 1. Main faults and deformational features of the New Madrid seismic zone (Odum et al., 1998; Purser and Van Arsdale, 1998). Arrows indicate fault displacement on strike-slip faults and teeth on the Reelfoot thrust fault point opposite fault propagation direction. "U" indicates the up-thrown and "D" indicates the down-thrown Reelfoot fault blocks. The Lake County uplift is a hanging wall anticline of the Reelfoot fault (Odum et al., 1998; Purser and Van Arsdale, 1998). Proposed kink bands (Purser and Van Arsdale, 1998) and tear faults (Odum et al., 1998) associated with this anticline are both shown. The Reelfoot scarp is a fault-propagation monoclinal fold developed along the fault front and enlarges proportional to Reelfoot fault displacement (Russ, 1982; Van Arsdale, 2000). Hatchures on the Reelfoot fault indicate slope from modern up-thrown to relative down-thrown fault-induced topography. Inset shows location of high-density epicenters within the New Madrid seismic zone (NMSZ), major surrounding faults, the boundary of the Mississippi embayment, and the principle regional intraplate stress vectors (after Zoback and Zoback, 1980).

Current methods have not confirmed any discrete pre-AD 900 Reelfoot slip events. Lack of pre-AD 900 warping in the surficial sediments draping the Reelfoot scarp further preclude any surficial deformation between the time of deposition for these strata (by 273 BC + 114/ − 69) and the AD 900 event (Guccione et al., 2002). The total structural relief accumulated at the stratigraphic base of the Holocene section at the scarp is a minimum of 15 m (Van Arsdale, 2000). Only 8–9 m of this relief is accounted by AD 900 and later events. Holocene slip events that predate strata preserved surficially above the scarp are, thus, implicit and are proposed in this paper.

3. Methods

3.1. Procedural concepts

Local influence of active faulting on modern alluvial river patterns and the sedimentary preservation of these tectonic effects are both well documented (Holbrook and Schumm, 1999; Schumm et al., 2000). Surficial warping where active faults traverse rivers will alter local floodplain gradient. This may force the channel to divert to tectonically lower topography. Where this is not preferable, the river will maintain position and traverse the surficial deformation. Traversing such surficial deformation will locally alter channel gradient (here defined as the slope of the channel thalweg) and, thus, stream power, causing the river to compensate for this change through a short list of predicted channel morphological responses and/or localized aggradation or incision (Fig. 2).

Response of a river to channel gradient deformation will depend on the pre-existing pattern of the river channel and the magnitude and direction of the imposed gradient alteration. This permits some prediction of tectonic response for specific river segments. For instance, the pattern change typically imposed on meandering rivers, like the Mississippi, by modest tectonic lowering of channel gradients is an overall reduction in sinuosity. This is because the kinetic energy needed to maintain wide meander loops is simultaneously reduced as gradient decreases (Ouchi, 1985; Schumm et al., 2000). More substantial decrease of gradient in meandering rivers may induce anastomosing patterns or swamps and lakes in extreme cases (Schumm et al., 2000). Straightening is the typical pattern response of the modern Mississippi channel to tectonic gradient decrease throughout its lower alluvial valley, which includes the study reach (Fig. 1) (Spitz and Schumm, 1997). In fact, the anomalously low sinuosity of the modern Mississippi River channel directly up dip of the New Madrid seismic zone has been previously attributed to 1812 uplift on the Reelfoot scarp and the related gradient reduction there imposed (Russ, 1982; Boyd and Schumm, 1995).

Aggradation can accompany straightening as a dual response to lowered channel gradients or may compensate fully for gradient change in cases where straightening is not feasible. Recent floodplain aggradation identified updip of the Reelfoot scarp is accordingly interpreted to be in response to scarp uplift (Guccione et al., 2002).

3.2. Procedure

Building on these concepts, we developed a paleoseismological approach that constrains past fault slip events by examining records of ancient channel deposits for prior evidence of abrupt fault control. The first step of this process entailed mapping of abandoned meander loops from the Holocene meander belt of the Mississippi River over a 100 km reach spanning the Reelfoot fault. Continued channel avulsion and meandering in sinuous river systems like the Mississippi tends to generate lithologically repetitive surficial strata that more often accrete laterally, instead of accumulate vertically, through time. This renders lithostratigraphy an insufficient mapping tool for discerning detailed channel history. We instead followed allostratigraphic techniques developed previously for the Lower Mississippi Valley by Autin (1992) and Saucier (1994). Allostratigraphic units mapped include channel-fills (which record abandoned channel courses), point bars (which reflect meander migration paths prior to channel abandonment), and crevasse splays (which reflect local aggradation of the floodplain after abrupt levee breach). An arcuate channel-fill segment and its enveloped point bar are identified as a channel-loop allounit, and collections of associated channel loops are mapped as allomembers or alloformations. Allounits were mapped by first identifying their characteristic surficial geometry on color infrared satellite imagery, air photos, and topographic maps. Then we tested these interpretations by confirming predicted characteristic lithofacies in the field through hand augering.

The second step entailed reconstruction of channel history from map data and assessment of these reconstructions for evidence of tectonic control. Specifically, we reconstructed representative channels for discrete time intervals, then identified shifts in pattern for these channels that are typically reflective of fault control (e.g., Fig. 2). Particular attention was directed toward detecting meander straightening responses. Channels were reconstructed based on the assumption that the abandoned channel in each meander loop records a segment of a local past course of the Mississippi River and that scrolls within point bars record lateral accretion trends of the channel prior to abandonment. We extrapolated linking channel reaches in between preserved coeval channel segments to form estimates of continuous time-representative channel courses. In reaches where preservation of loops or resolution of dates does not permit a unique channel location to be assessed for a specific time of reconstruction, a generalized pattern of the channel was estimated from morphologic trends in adjacent correlative loops. We concurrently identified any evidence of substantial river incision/aggradation or unusually dramatic changes in channel cross-sectional geometry that might also record a tectonic response.

Channel loop deposits were dated by cross-referencing relative (crosscutting relationships and soil development)

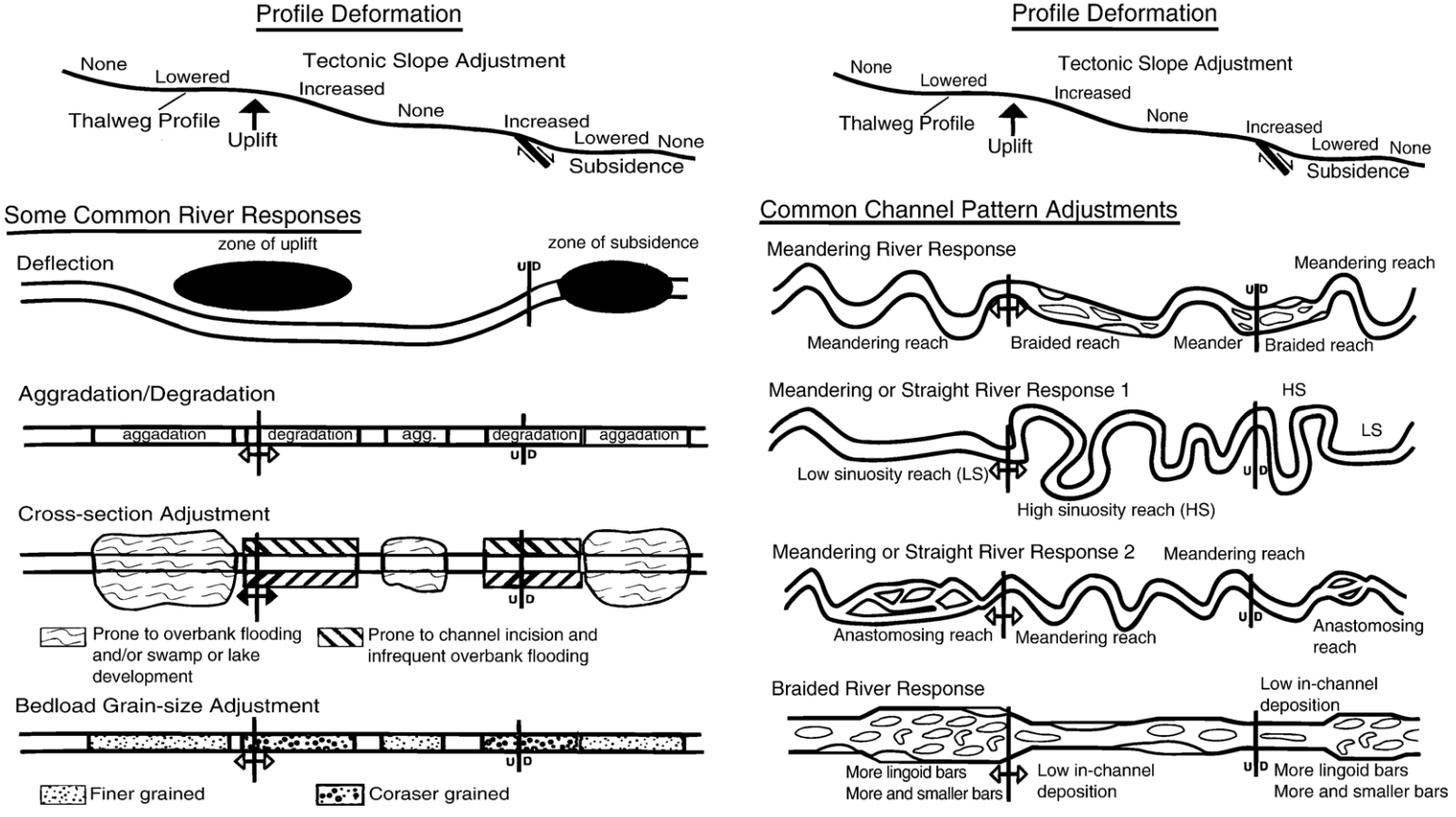

Fig. 2. Potential responses of rivers to gradient changes imposed by tectonic surficial warping. The left figure indicates four general tectonic responses, including simple deflection of the river from the deformed site. The right half of the figure depicts corresponding variations in channel pattern that may be caused by tectonic influence. The four responses on the left may occur concurrently with any response on the right, but the pattern responses on the right constitute a mutually exclusive set (Holbrook and Schumm, 1999).

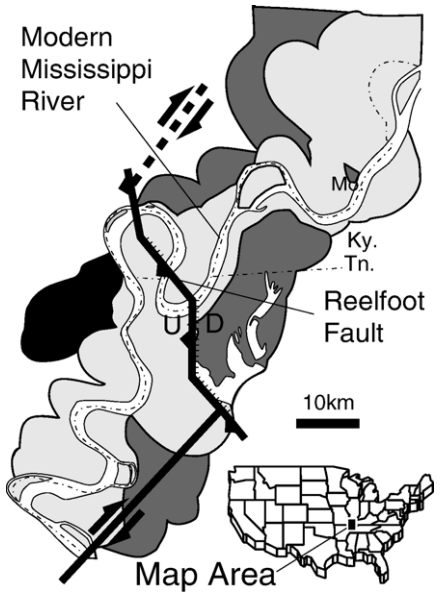

Fig. 3. Alloformations of Holocene Mississippi River strata across the New Madrid seismic zone. Initiation of the early/middle Holocene Portageville Alloformation (black) is uncertain, but the termination was near 4292 BC when the youngest contemporary channel was abandoned. The middle-Holocene Bondurant Alloformation (medium gray) begins at this time and continues until shortly after deposition of the youngest dated deposits in this plain (~1304 BC). The late-Holocene New Madrid Alloformation (light gray) begins before the abandonment of the oldest dated contemporary meander loop (~798 BC) and continues today. See Table 1 for further details regarding dates.

and numerical (calibrated radiocarbon [RC] and optically stimulated luminescence [OSL]) age estimates. Meander loops are assumed younger than loops that they crosscut, which facilitates relative sequencing of loops directly from allostratigraphic maps. Progressive soil development was considered to be evidence of relative age of bar surfaces where drainage and other soil-forming factors are otherwise similar (Aslan and Autin, 1998). Samples for numerical dates were collected under strict protocols in order to minimize spurious dates related to sampling errors. All numerical RC dates were collected following tested optimization strategies for meandering fluvial systems (Tornqvist and Van Dijk, 1993). RC samples are collected from the basal 15% of the fine-grained passive-channel fill, directly above the coarser active-channel fill. These RC dates record the time when abandonment-stage filling initiated, just after cut off of the channel from active river flow. All RC samples are of single fragments of taxonomically identified subaerial plant material extracted from anoxic lake muds and no unidentified organic fragments or samples with ambiguous stratigraphy were used. The organic samples processed were deposited in placid anoxic bottom water of the abandonment-phase oxbow-lake environment. The potential for introduction of older reworked material from stream transport during deposition, or younger surficial material from bioturbation and soil vertic processes, is thus considered minimal. All OSL ages were processed from 90 to 125 μ quartz collected from the upper 0.5–1.0 m of point bar sand beneath finer-grained deposits using an opaque sampling tube within a Gidding's probe coring system. Each OSL sample records the time during loop construction when lateral channel migration reached the sample site. OSL samples were cross-referenced against RC samples and crosscutting relationships to assure consistency. All OSL dates collected are used and prove to be consistent with other chronologic data. After OSL dating proved robust based on cross-check with other techniques, it was used independently to date some loops where RC dating protocols could not be met.

4. Holocene channel modification from Reelfoot fault slip events

The results of our mapping (Figs. 3, 4, and 5, and Table 1) record the first internally consistent numerical ages for a set of Lower Mississippi Valley meander loops. These data support assessment of two straightening responses on the Mississippi River, initiating in late (~ AD 900) and middle (~2200 BC to ~1600 BC) Holocene, respectively. These straightening responses are interpreted to reflect gradient loss owing to scarp uplift and are proxies for the beginning of two discrete millennial-scale intervals of repetitive slip on the Reelfoot fault. Continued river straightening, aggradation/incision responses, and/or channel diversion record river response to later events within these two slip intervals.

4.1. Late Holocene New Madrid Alloformation

4.1.1. Allostratigraphy and channel reconstructions

The Late Holocene New Madrid Alloformation records two informal allomembers, an older medium-sinuosity member, which records meandering throughout the map area, and a younger low-sinuosity member,

Fig. 4. Stratigraphy of the late-Holocene New Madrid Alloformation (A) and reconstructed channel courses (B) for the times before and after the ~AD 900 straightening response. Channel loops in (A) that were used for constructing the pre-straightening channel in (B) and the pre-straightening channel in (B) are both marked with the same hachured pattern.

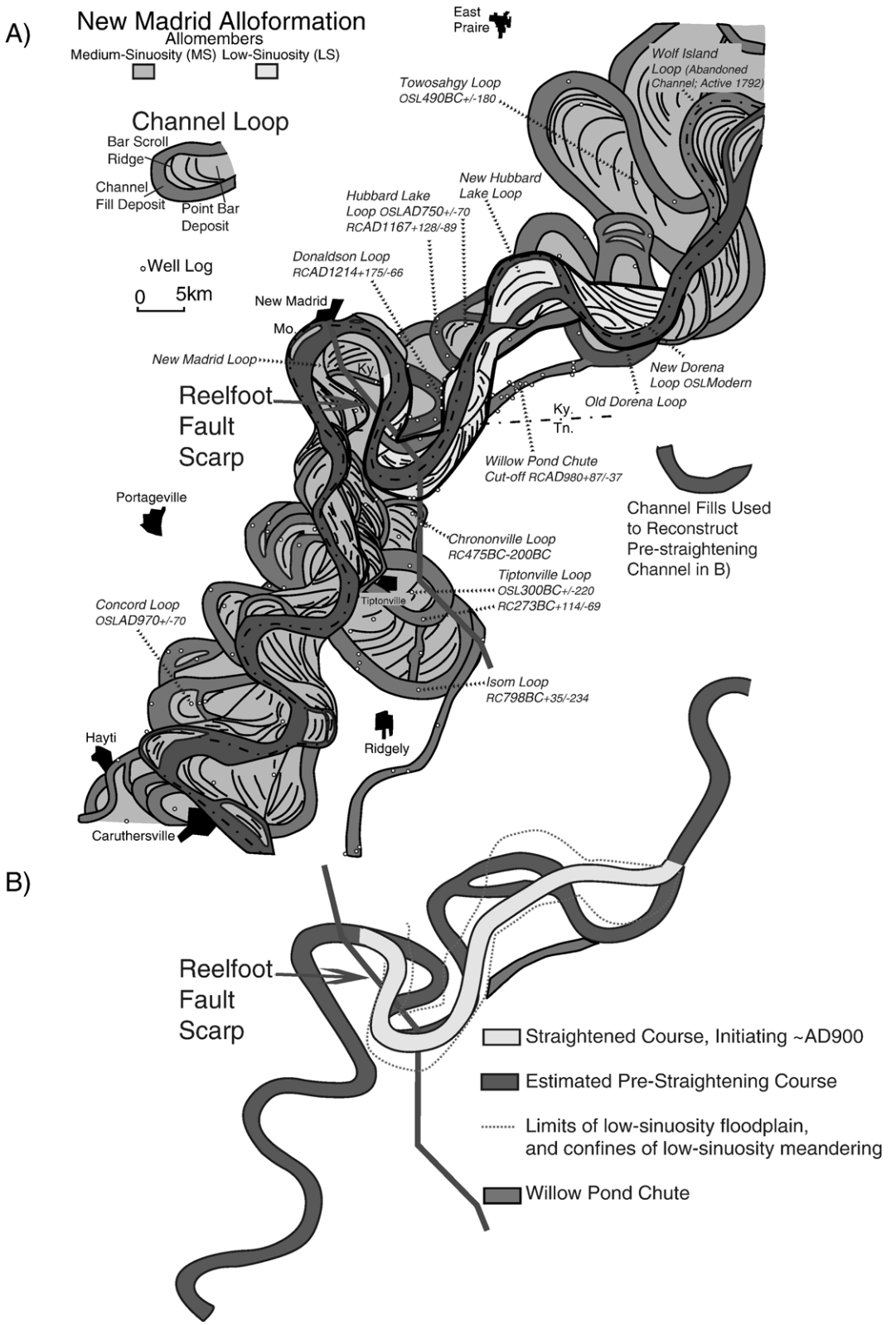
A)
New Madrid Alloformation
Allomembers
Medium-Sinuosity (MS) Low-Sinuosity (LS)
Channel Loop
Bar Scroll Ridge
Channel Fill Deposit
Point Bar Deposit
Well Log
0 5km
East Prairie
Towosahgy Loop OSL490BC+/-180
Wolf Island Loop (Abandoned Channel; Active 1792)
New Hubbard Lake Loop
Hubbard Lake Loop OSLAD750+/-70 RCAD1167+128/-89
Donaldson Loop RCAD1214+175/-66
New Madrid
Mo.
Ky.
New Madrid Loop
Reelfoot Fault Scarp
New Dorena Loop OSLModern
Old Dorena Loop
Ky.
Tn.
Willow Pond Chute Cut-off RCAD980+87/-37
Channel Fills Used to Reconstruct Pre-straightening Channel in B)
Portageville
Chrononville Loop RC475BC-200BC
Tiptonville Loop OSL300BC+/-220 RC273BC+114/-69
Tiptonville
Concord Loop OSLAD970+/-70
Isom Loop RC798BC+35/-234
Hayti
Ridgely
Caruthersville
B)
Reelfoot Fault Scarp
Straightened Course, Initiating ~AD900
Estimated Pre-Straightening Course
Limits of low-sinuosity floodplain, and confines of low-sinuosity meandering
Willow Pond Chute

which records local meander suppression following a straightening response at about AD 900 (Figs. 3 and 4). The medium-sinuosity member initiated after the abandonment of the middle-Holocene Bondurant Alloformation after 1304 BC±306 (Figs. 3 and 6 and Table 1) and continued until the initiation of the low-sinuosity member. At least seven medium-sinuosity loops are preserved in the reach adjacent to the younger low-sinuosity member (Fig. 4). The transition to the low-sinuosity member marks a short interval of time when the three youngest consecutive medium-sinuosity meander loops of these seven were cut off in rapid succession over a 30 km valley length. These loops are the Donaldson loop, Hubbard Lake loop, and Old Dorena loop/Willow Pond chute system (Fig. 6). Each of these loops were abandoned by chute cutoff because they each lacked sufficient curvature to bring channels on opposing sides of the meander into sufficiently close proximity for neck cutoff typical of very high-sinuosity meander loops. The segments which once linked these loops were eroded by later low-sinuosity meandering. The reconstructed course extrapolated through the Old Dorena, Hubbard Lake, and Donaldson loops constitutes an estimate of the Mississippi River channel prior to the straightening response which initiated the low-sinuosity member (Fig. 4B).

The river began this straightening response with abandonment of the Old Dorena loop/Willow Pond chute complex (Figs. 4 and 6). The Willow Pond chute received sufficient discharge from the Old Dorena loop to maintain a channel up to 1/4 the size of the contemporary main channel until both were abandoned by chute cutoff at AD 980+87/−37. The New Dorena loop initiated at this time. Cutoff of the Hubbard Lake loop began soon thereafter. The Hubbard Lake cutoff was completed shortly before AD 1167+128/−89, when oxbow lake deposits first began filling the abandoned channel. Cutoff of Donaldson loop followed in rapid succession and was completed by AD 1214+ 175/−66. The sequence of events that resulted in river straightening and initiation of river bypass through the current low-sinuosity member, thus, started at or shortly after AD 900 and was completed before AD 1214+175/−66.

The AD 900 straightening response established a low-sinuosity channel that maintains itself with minor modification to the modern day. The limits of the low-sinuosity allomember encompass all channels produced in the low-sinuosity floodplain since its inception; hence, the position of the initial low-sinuosity channel is limited by these confines. The position of the channel produced by the AD 900 straightening response is estimated in Fig. 4B by placing this channel at the location required for initiation of the point bars confined within the low-sinuosity floodplain. Considering sinuosity to equal the ratio between the channel length and the length of the meander axis, inception of the low-sinuosity channel as drawn constitutes a sinuosity drop from 1.6 (pre-AD 900 medium-sinuosity course) to 1.0. Sinuosity of the modern Mississippi channel has returned to 1.5 in the upstream half of the low-sinuosity member, approaching its prior medium-sinuosity form. The channel has not changed notably in the downstream half, where it has maintained a sinuosity of approximately 1.0 since inception. This modern sinuosity is representative of the maximum sinuosity the river could have acquired at anytime during or since straightening while still remaining within the confines of the low-sinuosity floodplain.

No indications of a similar period of straightening are recorded downstream or upstream of the low-sinuosity member, and meandering in both locations appears to have been continuous there throughout deposition of the New Madrid Alloformation (Fig. 4). Loops downstream are each of equal or greater amplitude to those medium-sinuosity loops adjacent to the low-sinuosity member and do not argue for a similar period of straightening maintained over a similarly extended reach. A representative sinuosity is presented for this reach based on the general form of preserved adjacent meanders, except for the segment that includes the Concord loop, where the morphology of the channel near AD 900 is reasonably known (Fig. 4B). The Towosahgy loop upstream of the low-sinuosity member is crosscut by a loop older than the Old Dorena loop; thus, the Towosahgy loop was abandoned, and the subsequent Wolf Island loop was initiated, well before the inception of the Old Dorena loop. The precise date of abandonment of the Wolf Island loop is uncertain, but the Wolf Island channel still maintained flow when the Missouri/Tennessee state line was drawn in AD 1792.

4.1.2. Tectonic interpretation

Spatial and temporal agreement between the ~ AD 900 straightening response and independent paleoseismic

Fig. 5. Stratigraphy of the middle-Holocene Bondurant Alloformation (A), and reconstructed channel courses (B) for the times before and after the straightening response that occurred between ~2200 BC and ~1600 BC. Channel loops in (A) used for constructing the pre-straightening channel in (B) and the pre-straightening channel in (B) are both marked with the same hachured pattern.

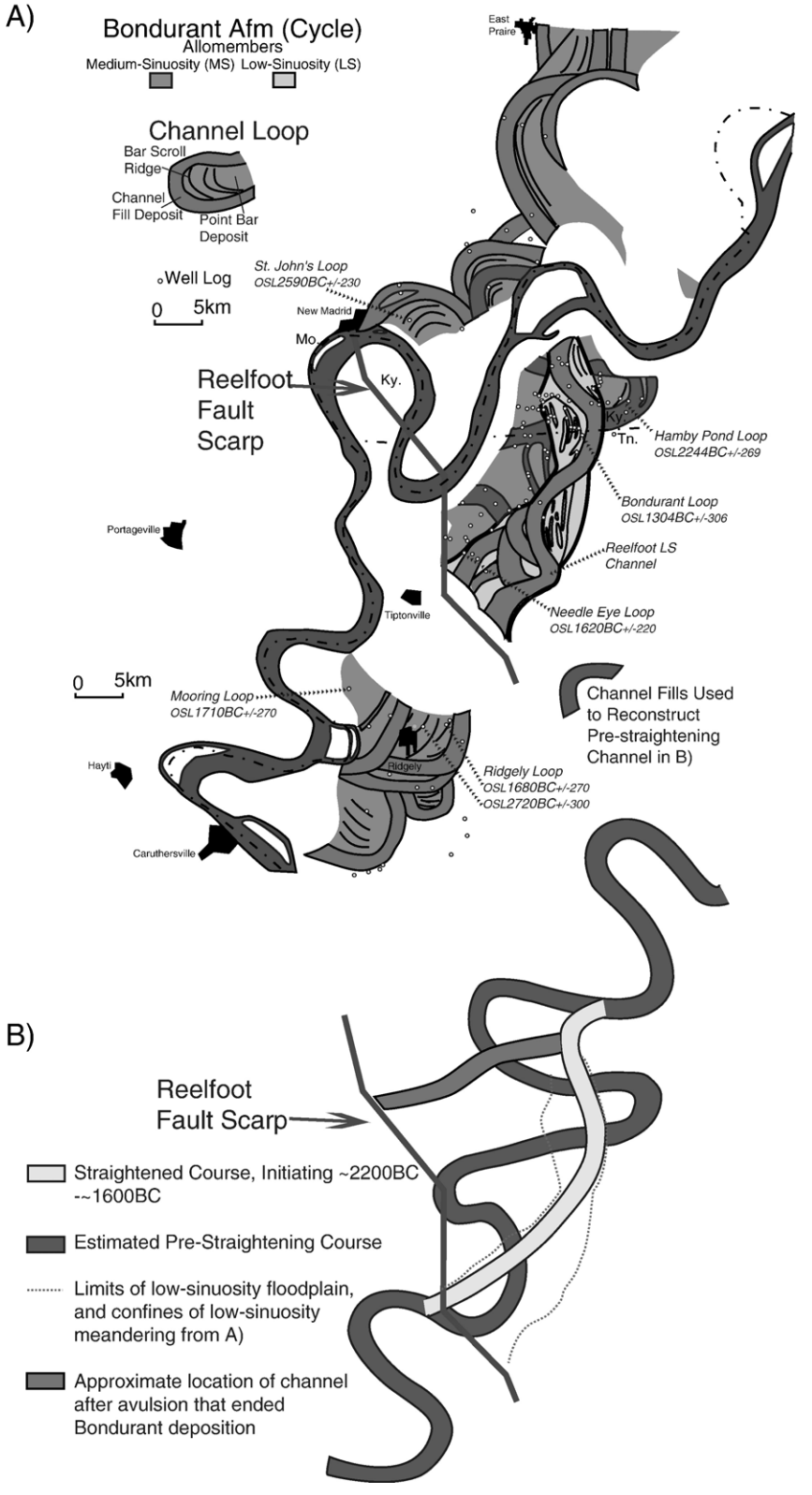
A)
Bondurant Afm (Cycle)
Allomembers
Medium-Sinuosity (MS) Low-Sinuosity (LS)
Channel Loop
Bar Scroll Ridge
Channel Fill Deposit
Point Bar Deposit
Well Log
0 5km
St. John's Loop
OSL2590BC+/-230
New Madrid
Mo.
Ky.
Reelfoot Fault Scarp
East Praire
Tn.
Hamby Pond Loop
OSL2244BC+/-269
Bondurant Loop
OSL1304BC+/-306
Reelfoot LS Channel
Needle Eye Loop
OSL1620BC+/-220
Portageville
Tiptonville
Mooring Loop
OSL1710BC+/-270
Channel Fills Used to Reconstruct Pre-straightening Channel in B)
Hayti
Ridgely
Ridgely Loop
OSL1680BC+/-270
OSL2720BC+/-300
Caruthersville
B)
Reelfoot Fault Scarp
Straightened Course, Initiating ~2200BC -~1600BC
Estimated Pre-Straightening Course
Limits of low-sinuosity floodplain, and confines of low-sinuosity meandering from A)
Approximate location of channel after avulsion that ended Bondurant deposition

evidence for surficial deformation (Russ, 1982; Kelson et al., 1996; Guccione et al., 2002; Tuttle et al., 2002) argues that this straightening records channel gradient decrease caused by the previously recognized AD 900 Reelfoot fault slip event. Cutoff of the three consecutive meander loops that resulted in river-channel straightening began just after the AD 900 slip event. Straightening at that time is also confined to the 30 km reach directly upstream of the Reelfoot scarp, where gradients were diminished by fault-induced uplift (Fig. 4). Meanders were maintained elsewhere along the river, where gradients were increased or unchanged.

The total amount of uplift generated over the Lake County uplift during the AD 900 event is not rigorously quantified. Prior workers (e.g., Van Arsdale, 2000) have estimated AD 900 uplift at the Reelfoot scarp proper to be approximately 2.7 m based on the assumption that the AD 900, AD 1450, and AD 1812 slip events each generated approximately equal surficial deformation. Direct observations from trenches and surficial drainages at the scarp, however, suggests that the AD 900 event caused less scarp uplift than subsequent AD 1450 (approx. 3–4 m) and AD 1812 (approx. 3–4 m) events (Kelson et al., 1996; Guccione et al., 2002; Guccione, 2005). Based on these estimates, a scarp uplift of approximately 1m seems to be a reasonable and conservative first approximation for the AD 900 event. An estimated 1m of uplift would have reduced gradient

Table 1
(a) Dates and significance from allounits in the Mississippi River deposits of the New Madrid seismic zone

Allounit and sample lab #	Material dated[a]	Landscape and stratigraphic position	Depositional event dated	Age (years b.p.)	Dating method[b]	Calendar date[c]
New Madrid Alloformation						
Towosahgy Meander loop (UNL-863)	Fine sand	12 km from point bar apex; upper 0.5 m of well-sorted sand beneath 4.0 m of mixed clay and loamy sand.	Point bar deposition near initiation of point-bar growth	2490+/−180	OSL	490 B.C. +/−180
New Dorena point bar (MCB-03-28-10)	Fine sand	Adjacent to modern river; upper 0.5 m of section	Most recent episode of sandy point bar deposition	Modern	OSL	Modern
Hubbard Lake meander loop (A-0110)	Tree limb segment with leaf attachment	Mostly filled abandoned channel loop at south end of oxbow lake; 6.8 m below top and 1.6 m above base of muddy channel fill	Oxbow lake mud deposition after meander abandonment and 1.6 m of lake filling	872+/−34	RC	A.D. 1167 +128/ −89
Hubbard Lake point bar (UNL-046)	Fine sand	1.9 km from point bar apex; upper 0.5 m of well-sorted sand beneath 2.1 m of finer bar-top strata	Point bar deposition at initiation of final 1.9 km of point bar growth	1250+/−70	OSL	A.D. 750 +/−70
Donaldson meander loop (A-0090)	Unabraided charcoal	Filled abandoned channel loop; within clay at base of 1 m of mud fill; below 3.6 m of splay sand and silt; above sand and silt channel fill	Oxbow lake mud deposition after meander abandonment and before splay deposition into channel	844+/−49	RC	A.D. 1214 +175/ −66
Willow Pond chute channel (A-0025)	Unabraided charcoal	Filled chute channel; at base of 2.6 m section of silty-clay fill above loamy fine-sand fill	Abandonment of chute cut off between Old Dorena loop and modern channel; concurrent with abandonment of Old Dorena loop	1086+/−25	RC	A.D. 980 +87/ −37
Chrononville meander loop[d]	Charcoal	Extracted from point bar deposit within excavated trench across Reelfoot scarp in terminus of point bar	Time just before beginning of abandonment of meander loop	—	RC	476–200 B.C.

Table 1 (*continued*)

Allounit and sample lab #	Material dated[a]	Landscape and stratigraphic position	Depositional event dated	Age (years b.p.)	Dating method[b]	Calendar date[c]
Tiptonville meander loop[e]	Fine organic detritus	Filled abandoned channel loop; beneath mud fill, and within underlying silt and sand	Prior to meander abandonment at end of channel occupation	2240+/−20	RC	273 B.C.+114/−69
Tiptonville point bar (UNL-045)	Fine sand	2.1 km from point-bar apex; upper 0.5 m of well-sorted sand beneath 1 m of finer bar-top strata	Point bar deposition at initiation of final 2.1 km of point bar growth	2300+/−220	OSL	300 B.C. +/−220
Isom meander loop (A-4411)	Tree limb fragment with two stem attachments	Filled abandoned channel loop; within clay 5.8 m down into 7.4 m section of clay fill above loamy fill	Oxbow lake mud deposition after meander abandonment and 1.6 m of lake filling	2450+/−70	RC	532 B.C.+264/−140
Isom meander loop (A-0087)	Tree limb fragment with limb cell structure	Filled abandoned channel loop; within clay 7.0 m down into 7.4 m section of clay fill above loamy fill	Oxbow lake mud deposition after meander abandonment and 0.4 m of lake filling	2606+/−51	RC	798 B.C.+35/−234
Concord meander loop (UNL-847)	Fine sand	2.1 km from point-bar apex; upper 1 m of well-sorted sand beneath 0.8 m of finer bar-top strata	Point bar deposition at initiation of final 2.1 km of point bar growth	1030+/−70	OSL	A.D. 970+/−70
Bondurant Alloformation						
Reelfoot LS channel (A-0089)	Unabraided charcoal	Abandoned channel course; within fine sand 7.9 m down into >8.0 m section of mixed clay, silt, and sand fill	Last reoccupation of channel course; minimum date of channel abandonment	1325+/−49	RC	A.D. 679+38/−120
Reelfoot LS channel (A-0091)	Unabraided charcoal	Abandoned channel course; within silty clay 7.4 m down into >7.7 m section of mixed clay, silt, and sand fill	Last reoccupation of channel course; minimum date of channel abandonment	1756+/−48	RC	A.D. 302+170/−108
Bondurant point bar (UNL-314)	Fine sand	Approximate point-bar apex; upper 0.5 m of well-sorted sand beneath 3.2 m of finer bar-top strata	End of point-bar growth; avulsion of Reelfoot channel	3304+/−306	OSL	1304 B.C. +/−306
Hamby Pond point bar (UNL-313)	Fine sand	1.1 km from point-bar apex; upper 0.5 m of well-sorted sand beneath 2.1 m of finer bar-top strata	Point bar deposition at initiation of final 1.1 km of point bar growth	4244+/−269	OSL	2244 B.C.+/−269
Hamby Pond meander loop (A-0178)	Tree limb with stem bifurcation	Filled abandoned channel loop; within clay 6.4 m down into a 7.3 m section of mixed clay silt and loam fill	Last reoccupation of channel course; minimum date of channel abandonment	2591+/−49	RC	796 B.C.+33/−242
St John's meander loop (UNL-340)	Fine sand	1.6 km from point-bar apex; upper 0.5 m of well-sorted sand beneath 2.1 m of finer bar-top strata	Point bar deposition at initiation of final 1.6 km of point bar growth	4590+/−230	OSL	2590 B.C. +/−230
Needle Eye meander loop (UNL-829)	Very fine sand	Initial scour of point bar in upper 1 m of fine sand beneath 5.5 m of mixed splay sand and mud veneer	Some unknown point in time during growth period of point bar	3620+/−220	OSL	1620 B.C. +/−220

(continued on next page)

Table 1 (*continued*)

Allounit and sample lab #	Material dated[a]	Landscape and stratigraphic position	Depositional event dated	Age (years b.p.)	Dating method[b]	Calendar date[c]
Mooring meander	Fine sand	5.5 km from point-bar apex; upper 0.5 m of well-sorted sand beneath	Point bar deposition at initiation of final	3710+/−270	OSL	1710 B.C. +/−270
Morring loop (UNL-833)		4.1 m of finer bar-top strata	5.5 km of point bar growth			
Ridgely meander loop (UNL-832)	Fine sand	2.7 km from point-bar apex; upper 1 m of well-sorted sand beneath 4.2 m of finer bar-top strata	Point bar deposition at initiation of final 2.7 km of point bar growth	4720+/−300	OSL	2720 B.C. +/−300
Ridgely meander loop (UNL-830)	Fine sand	0.2 km from point-bar apex; upper 2 m of well-sorted sand beneath 2.1 m of finer bar-top strata	Point bar deposition at initiation of final 0.2 km of point bar growth	3680+/−270	OSL	1680 B.C. +/−270
Portageville Alloformation						
Portageville LS channel (A-0088)	Tree limb segment with gymnosperm limb cell structure	Abandoned channel course; within clay 5.9 m down into >8.2 m section of mixed clay, silt, and loam fill	Last reoccupation of channel course; minimum date of channel abandonment	3754+/−50	RC	2172 B.C. +131/ −190
Portageville LS channel (A-0093)	Single seed (c.f., grass seed)	Abandoned channel course; within clay 6.0 m down into >8.2 m section of mixed clay, silt, and loam fill	Last reoccupation of channel course; minimum date of channel abandonment	5414+/−60	RC	4292 B.C. +65/−245
Point Pleasant meander loop (UNL-341)	Fine sand	Near point bar apex; upper 0.5 m of well-sorted sand beneath 2.3 m of finer bar-top strata	Point bar deposition near final stages of point bar growth during Portageville meander phase	7250+/−360	OSL	5250 B.C. +/−360
Portageville point bar (UNL-172)	Fine sand	4.3 km from point-bar apex; upper 0.5 m of well-sorted sand beneath 1.5 m of finer bar-top strata	Point bar deposition at initiation of final 4.3 km of point bar growth	7484+/−367	OSL	5484 B.C. +/−367

(b) Optical age analysis from point-bar sand (analysis performed at the University of Nebraska-Lincoln, Department of Geosciences)

Sample number	UNL lab number	Point-bar allounit	Dose rate (Gy/ka)	No. of aliquots	De (Gy)	Optical age (ka)
New Madrid Alloformation						
LC400	UNL-863	Towosahgy	1.96±0.11	33	4.89±0.15	2.49±0.18
MCB 03-28-8	UNL-046	Hubbard Lake	2.24±0.09	24	2.79±0.12	1.25±0.07
MCB 03-26-1	UNL-045	Tiptonville	1.37±0.05	20	3.16±0.29	2.30±0.22
RL67	UNL-847	Concord	1.71±0.09	34	1.76±0.07	1.03±0.07
Bondurant Alloformation						
MCB 01-13-13	UNL-314	Bondurant	1.94±0.14	18	6.42±0.33	3.30±0.31
MCB 01-13-12	UNL-313	Hamby Pond	1.46±0.08	20	6.19±0.27	4.24±0.27
MCB 01-15-15	UNL-340	St. John's	2.49±0.10	26	11.43±0.42	4.59±0.23
LC-99	UNL-829	Needle Eye	2.15±0.11	34	7.76±0.22	3.62±0.22
LC1266	UNL-833	Mooring	2.14±0.13	31	7.96±0.25	3.71±0.27
LC966	UNL-832	Ridgely	1.56±0.07	30	7.34±0.29	4.72±0.30
LC96	UNL-830	Ridgely	2.32±0.15	29	8.53±0.18	3.68±0.27
Portageville Alloformation						
MCB 01-15-16	UNL-341	Point Pleasant	1.66±0.07	21	12.03±0.39	7.25±0.36
MCB 03-28-2	UNL-172	Portageville	2.12±0.10	23	15.81±0.57	7.48±0.37

Table 1 (*continued*)
(c) Dose-rate data for optical ages

Sample number	UNL lab number	Depth (m)	H_20 (wt.%)	U (ppm)	Th (ppm)	K_2O (wt.%)	Cosmic (Gy/ka)	Dose rate (Gy/ka)
MCB 03-26-1	UNL-045	2.3	1.6±0.5	0.63±0.1	1.9±0.2	1.19±0.03	0.16	1.37±0.05
MCB 03-28-2	UNL-172	1.8	13.2±4.0	1.84±0.13	6.54±0.59	1.73±0.04	0.17	2.12±0.10
MCB 03-28-8	UNL-046	2.4	5.1±1.5	1.65±0.1	6.25±0.6	1.71±0.04	0.15	2.24±0.09
MCB 01-13-12	UNL-313	2.7	15.6±4.7	0.9±0.1	3.2±0.3	1.43±0.04	0.15	1.46±0.08
MCB 01-13-13	UNL-314	3.7	28.5±8.6	1.7±0.1	8.0±0.7	1.89±0.05	0.13	1.94±0.14
MCB 01-15-15	UNL-340	2.4	5.5±1.7	1.7±0.1	8.2±0.7	1.88±0.05	0.15	2.49±0.10
MCB 01-15-16	UNL-341	3.0	8.0±2.4	0.9±0.1	4.6±0.4	1.42±0.04	0.14	1.66±0.07
LC-99	UNL-829	6.6	21.4±6.4	1.6±0.1	6.9±0.6	2.07±0.04	0.09	2.15±0.11
LC96	UNL-830	3.7	33.4±10.0	2.1±0.1	9.2±0.8	2.34±0.05	0.13	2.32±0.15
LC966	UNL-832	4.6	9.6±2.9	0.8±0.1	3.1±0.3	1.45±0.04	0.12	1.56±0.07
LC1266	UNL-833	4.6	29.8±8.9	1.7±0.1	8.8±0.8	2.11±0.04	0.12	2.14±0.13
RL67	UNL-847	1.7	22.4±6.7	1.1±0.1	4.7±0.4	1.67±0.04	0.17	1.71±0.09
LC400	UNL-863	4.6	27.7±8.3	1.6±0.1	6.8±0.6	1.95±0.04	0.12	1.96±0.11

[a] Plant taxonomic identification by Professor Alan Bornstien, Department of Biology, Southeast Missouri State University.

[b] Numerical age estimates by radiocarbon (RC) and optically stimulated luminescence (OSL) techniques. All RC dates were collected following tested optimization strategies (Tornqvist and Van Dijk, 1993). RC samples are from the basal 15% of the fine-grained, passive channel fill directly above the coarse, active channel fill, and record channel abandonment by active flow and initiation of abandonment-stage fill. All RC ages are of single samples of taxonomically identified subaerial plant material; no unidentified organic fragments or samples with ambiguous stratigraphy were used. All RC samples were processed at the Illinois Geological Survey. All OSL ages were processed at the University of Nebraska Geochronology Lab from 90–125 μ quartz collected from the upper 0.5-m of point-bar sand beneath finer-grained deposits and record the time when lateral channel migration reached the sample site.

[c] Radiocarbon ages calibrated to calendar dates B.P. using "CALIB" calibration program, and are reported at two sigma (Reimer et al., 2004). OSL ages are reported as years before collection, with sample collection in 2000, and reported at one sigma.

[d] Data from Kelson et al., 1996, Multiple late Holocene earthquakes along the Reelfoot fault, central New Madrid seismic zone: Journal of Geophysical Research, v.101, B3, p. 6151–6170.

[e] Data from Guccione et al., 2002, Stream response to repeated coseismic folding, Tiptonville dome, New Madrid seismic zone: Geomorphology v. 43, p. 313–49.

by about 22% over the straightened valley reach based upon the pre-AD 900 slope reconstructed by Russ (1982). Comparable river straightening is documented elsewhere along the modern Mississippi River in response to as low as 14% local gradient reduction (Spitz and Schumm, 1997). Uplift of 1 m, or even less, at either the Reelfoot scarp or over the broader Lake County uplift appears to be sufficient to induce the projected sinuosity response.

The sequence for cutoff of meanders during tectonically induced straightening should be controlled by two factors, namely the backwater effect caused by local obstructing uplift and the distribution of preferred breaching sites caused by local bank instabilities. Intuitively, the backwater effect should diminish progressively up valley and should thus favor cutoff of meanders beginning near the uplift, where the effect is most intensive, and proceeding upstream over time. The fact that the Old Dorena, Hubbard Lake and Donaldson Point chute cutoffs occurred in the reverse order argues that bank instability may have been a more important factor in determining the sequence of loop cutoff across the tectonically affected reach. Alternatively, the long-term meander response to tectonically generated backwaters may not always work as generally assumed. For instance, long-term loop cutoff trends may preferentially initiate well up stream from an uplift where the backwater effect is first encountered by the river because this is also the site where the backwater-related drop in bed-load transport capacity is first encountered. In-channel aggradation that could prompt chute cutoff would likely migrate progressively from this point downstream toward the uplift. This sedimentation-driven model would be one possible explanation for the downstream progression of chute cutoffs observed.

Tectonic channel straightening for the Mississippi River was not necessarily instantaneous and likely required decades to centuries to complete. Rapidity of the tectonic straightening response is uncertain, but is confined to sometime within a ~300-year window, starting near AD 900. This, however, is well before the subsequent (AD 1450) uplift event and constitutes a rapid change compared to the minimal amount of re-growth and cutoff of meanders in this reach during the 800–1100 years since (Fig. 4).

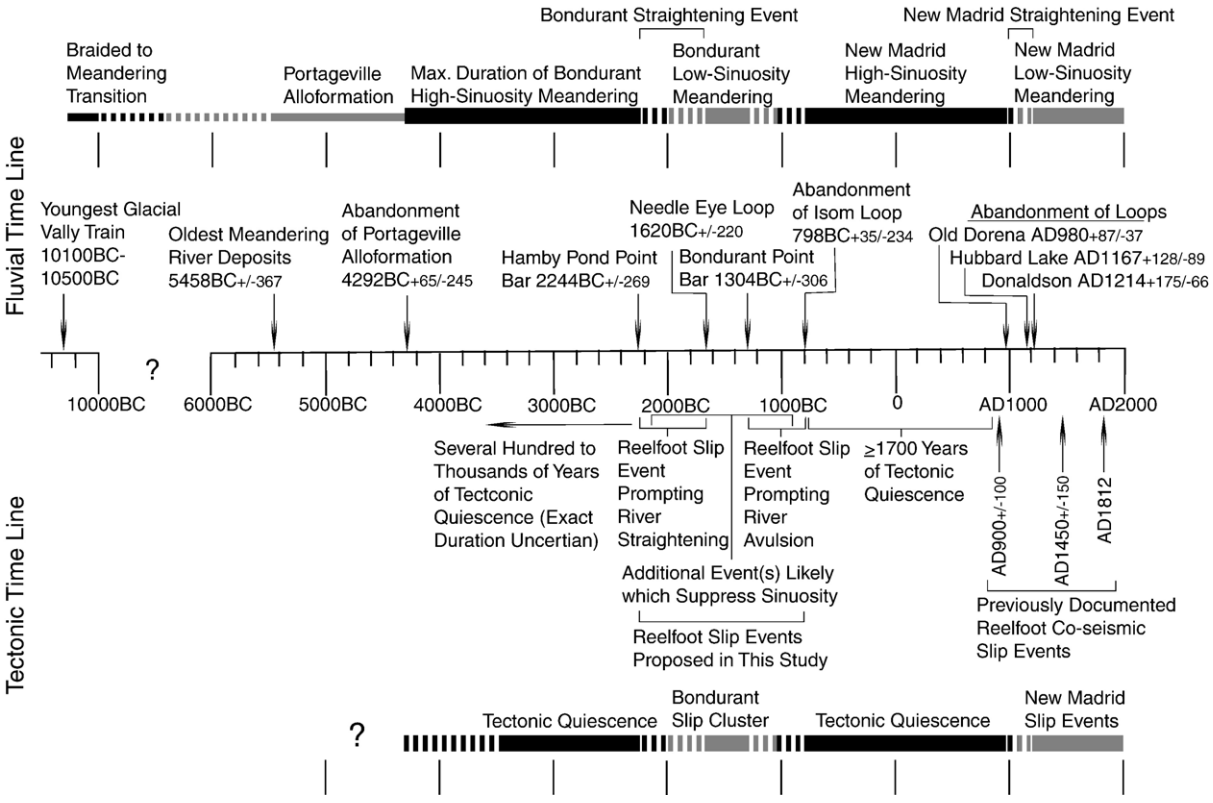

Fig. 6. Summary of fluvial responses and interpreted tectonic events for the middle- and late-Holocene Reelfoot Fault. Previously documented AD 900 and later slip events are discussed in Russ (1982), Kelson et al. (1996), and Guccione et al. (2002). Timing presented for medium- and low-sinuosity phases and related interpretations for tectonic events are based on dates provided for the river responses that are placed along the center time graph. Timing for events is, thus, subject to the error range of these dates.

Scarp uplift and gradient reduction imposed by later co-seismic slip events (AD 1450 and AD 1812) were compensated mostly by scarp incision and scarp-front aggradation (Guccione et al., 2002; Holbrook et al., 2002), as further straightening of the previously straightened reach was no longer an effective river response. Splays developed around the front of the Reelfoot scarp and locally aggraded the floodplain here up to 2 m. Strata above the scarp were concurrently incised locally up to 10 m. This helped re-level the tectonically warped channel gradient. Some of these splay deposits poured into the oxbow lake of the previously abandoned Donaldson loop, where they are stratigraphically above approximately 1 m of post-abandonment, muddy, lake-fill deposits. The time of initial splaying is, thus, well after the abandonment of Donaldson loop that followed AD 900 uplift. The oldest dates for these splay deposits are AD 1430–1650 (Kelson et al., 1996), which lead Kelson et al. (1996) and Guccione et al. (2002) to interpret these strata to record initiation of scarp-front sedimentation in response to the AD 1450 slip event. The splay deposits are also split consistently in roughly the middle by a mollic A horizon. This argues that the splay complex was deposited during two short intervals, with sufficient time between events for modest soil development. The second/upper splay interval likely records a second tectonically induced splay episode in response to AD 1812 co-seismic slip well after the AD 1450 splay was completed. The numerical dates to confirm this assertion, however, are currently unavailable.

In addition to causing scarp-front aggradation, the later AD 1450 and AD 1812 slip events maintained a reduced gradient in the low-sinuosity reach and inhibited the re-growth of meander loops there to pre-AD 900 amplitudes. This forced continuation of the much reduced sinuosity established after AD 900 until the present day, at least in the lower half of this river segment (Fig. 4). Recent cutoff of the Wolf Island loop may also be related to maintenance/expansion of straightening after the AD 1812 earthquake event, as Russ (1982) suggested. Such reinforcement of straightening could also explain the ongoing cutoff attempt of the New Hubbard Lake loop (Fig. 4A). AD 1812 uplift

Table 2
Representative meander rates from meander loops within the study reach

Loop Name	Meander rate[a]	Comments
New Dorena	5.4 m/yr (5.2–5.8 m/yr)	Considers initiation of this meander as time of Willow Pond chute abandonment, and all 5500 m of growth from then to present is considered.
New Hubbard Lake	7.6 m/yr (6.7–8.6 m/yr)	Considers 6400 m of total meander enlargement since its inception after the cutoff of Hubbard Lake loop.
Hubbard Lake	4.8 m/yr (3.5–7.8 m/yr)	Considers 2000 m of total meander enlargement from position of OSL age to abandonment of meander. Rate thus includes the time required for channel abandonment.
New Madrid loop	4.0 m/yr (3.8–5.2 m/yr)	Considers that part of the growth of the meander that has occurred to date from the position of the meander projected from Donaldson loop prior to abandonment (3200 m), and considers date of Donaldson loop abandonment as beginning if this meandering. (Boyd and Schumm (1995) noted that migration of this loop was impeded by resistant strata of Sikeston Ridge at its apex.)
Tiptonville	81 m/yr (7.1 m/yr–instantaneous)	Considers 2200 m of total meander growth from position of OSL age to abandonment of meander. Rate thus includes the time required for channel abandonment. (Rates for meanders with strong curvature, like the Tiptonville, commonly have rates up to an order of magnitude higher than more open meanders in this reach of the Mississippi River during historic times (Hudson and Kesel, 2000).)
Ridgely Meander	2.5 m/yr (1.5–5.3 m/yr)	Considers the 2500 m of total meander growth between the two OSL dates collected within this single meander loop.
Four modern meander loops between Tipptonville, TN and Caruthersville, MO	12 m/yr (9–15 m/yr)	Based on general comparison between estimates of the historic 1812 channel position and the modern Mississippi River (see Odum et al., 1998). Records two-century-averaged rate for reach that sits above and abruptly downstream of the place where gradient was tectonically steepened by 1812 elevation of the Lake County uplift.
All meanders from the apex of the lower Mississippi Valley at Cairo, Illinois south for 825 valley km during the pre-modification period of the channel between 1877 and 1924	Approx. 30 m/yr with a range from approx. 10 to 65 m/yr	Measurement constitutes an average of maximum meander rates for the Mississippi River within this reach (which includes the study reach) as measured from historic river surveys by Hudson and Kesel (2000). Rates were measured by finding the local points reflecting maximum bar accretion between surveys, and then dividing this difference by the number of years between the surveys. Their actual cited average is 38.4 m/yr, but this includes three loops with anomalously rapid meander rates topping 80 m/yr. Anomalously rapid meander rates are noted by these authors to coincide with meanders with very high curvature (c.f., Tiptonville, Isom, and Towosahgy loops). With these loops excluded, average meander rates over this period are closer to the numbers indicated. These rates offer an estimate of faster short-term accretion of local bar segments, whereas prehistoric rates from this study reflect the slower long-term accretion and preservation rates of entire bar complexes.

Table includes both long-term migration rates from numerical estimates, and short-term meander rates from historical data.
[a] Meander rate = maximum point bar width / meander duration.

also blocked the Running Reelfoot channel east of the main Mississippi River, and caused water to backup and fill the lower topography above the Bondurant low-sinuosity member (see next section) to form Reelfoot Lake (Figs. 1 and 5).

Just as loss of slope will tend to decrease sinuosity, increases in slope will tend to increase sinuosity. Increased meandering should thus be generated around the steepened downstream slope of Lake County uplift as a result of uplift events. This is the case; however, this response is not as apparent as the straightening response for two reasons. First, the hanging-wall anticline surficially manifest as the Lake County uplift has a series of active tear faults (Odum et al., 1998) or backthrusts (Purser and Van Arsdale, 1998) which generated uplift during the AD 1812 event approximately 16 km downstream of the town of New Madrid (Fig. 1). This secondary uplift on the top of the Lake County uplift muted sinuosity for a short reach across the crest of the uplift after AD 1812, and likely did so earlier as well. The four modern meander loops from here downstream to Caruthersville record the expected increased stream power gained from locally increased slope (Figs. 1 and 4). Comparisons between the modern channel and

estimates of the 1812 channel position (see Odum et al., 1998; Fig. 3) infer a sinuosity increase from about 1.4 to about 1.7 over this four-loop reach during the past two centuries in response to the most recent uplift event. A comparable sinuosity increase is not observed over any other reach in the mapped area. These data also suggest an approximate doubling of typical long-term meander rates to 12+/−3 m/yr for these four meanders. The measurement interval, however, is short, which gives reason to question whether some of this rate increase may be skewed by inclusion of faster short-term meander rates (Table 2).

A second reason why the predicted sinuosity increase is less apparent is because the increased-sinuosity response is temporally and physically less distinctive than the straightening response. Sinuosity increase is a slow constructive process limited in rate by the time required to accrete new point-bar complex. For instance, a 50% amplitude increase for a typical 6000 m-amplitude late-Holocene meander loop would require approximately 250 to 600 yr to complete, given an accelerated 12 m/yr rate verses a more regionally typical rate of 5 m/yr (Table 2). Such a slow growth rate suggests that the full increase in sinuosity initiated by AD 1812 uplift is likely still not realized even today, and the response to AD 1450 uplift may be incomplete as well. Tectonic sinuosity increase is also hard to demonstrate statistically. A typical individual meander with even a hypothetical amplitude increase of 50% (i.e. to 9000 m) might still prove difficult to distinguish from other still larger meanders occurring regularly and somewhat randomly over the valley (e.g., Isom loop, Towosahgy loop, Concord loop, etc.; Fig. 4). Likewise, while the increase in sinuosity from 1.4 to 1.7 observed locally after the 1812 earthquake is noteworthy, 1.7 in itself is not an anomalously high sinuosity for the Lower Mississippi River Valley. Alternatively, straightening is a high-amplitude and destructive response that is only limited in duration by the time required to cut a new channel and to plug the ends of abandoned channel loops. Straightening can thus rearrange channel pattern in a much more noticeable and comparatively abrupt way. The straightening response thus appears to be a more easily distinguishable and a more temporally discrete proxy than sinuosity increase for defining fault-slip events.

Trenching in late Holocene (~273 BC+114/−69 and younger; Guccione et al., 2002) sediments along the scarp-draping Chrononville loop (Fig. 4A) indicates that fault-induced uplift was minor or nonexistent during the ~1200 years prior to AD 900 (Russ, 1982; Kelson et al., 1996; Guccione et al., 2002). This assertion is based on age estimates of first-deformed sediments and the assumption that any pre-Chrononville topography on the scarp was beveled by Chrononville loop migration. Lack of relief between the Chrononville, Tiptonville, and Isom scarp-draping loops infer that this phase of inactivity extends to at least ~1700 years prior to the AD 900 event, when the oldest of these loops (Isom) was abandoned (798 BC+35/−234; Fig. 4A; Table 1). Importantly, meandering continued over the entire study reach and no straightening or analogous tectonic river response is apparent for this >1700 year period. Interpretations from this study are, thus, in agreement with prior paleoseismic studies that forward relative fault quiescence for this time interval.

4.2. Middle Holocene Bondurant Alloformation

4.2.1. Allostratigraphy and channel reconstructions

The middle Holocene Bondurant Alloformation also records two informal allomembers, which similarly record an early medium-sinuosity meandering phase that was followed by a localized straightening response with subsequent meander suppression (Figs. 3, 5 and 6). The medium-sinuosity member initiated after the abandonment of the Portageville Alloformation (4292 BC+65/−245; Figs 3 and 6 and Table 1) and continued until the initiation of the low-sinuosity member. Six medium-sinuosity loop remnants are preserved in the reach adjacent to the subsequent low-sinuosity floodplain. The youngest four of these six medium-sinuosity loops are not sufficiently preserved to foster direct dating of loop abandonment (Fig. 5A); thus, the duration for this straightening response is hard to assess directly. Stratigraphic differences between the low-sinuosity and medium-sinuosity member, however, are very distinct and argue for an abrupt and enduring change. First, the entire middle-Holocene low-sinuosity surface is uniformly incised 1.5 m below the adjacent and precursory medium-sinuosity surface. Straightening and initiation of the low-sinuosity member was, thus, coupled with uniform incision that postdated the medium-sinuosity surface, but was completed before preservation of low-sinuosity meandering. Second, low-sinuosity meandering lasted sufficiently to produce nine loops, each under 1/3 the amplitude of the precursory and adjacent medium-sinuosity meanders (Fig. 5A). The low-sinuosity member, thus, records a distinct meander history initiated by a major event that triggered a protracted local decline in meander amplitude and sinuosity.

The pre-straightening channel is reconstructed in similar fashion to the analogous pre-straightening channel of the New Madrid Alloformation (Fig. 5). The youngest four consecutive meander loops preserved in

the medium-sinuosity member that are cut by the low-sinuosity member were threaded together through the shortest reasonable course through younger segments. We assumed the minimal channel length with consistent meander curvature through the truncated reaches in order to produce a minimum estimate of channel sinuosity.

The range of potential shapes for the initial low-sinuosity channel that formed during the Bondurant straightening response can be reasonably constrained from preserved loops. The medium-sinuosity Ridgeley loop down valley of the low-sinuosity member shows a history of continual meandering throughout the time interval within which straightening occurred (see below). The adjacent and overlapping Mooring loop records approximately 5.5 km of subsequent lateral accretion, presumably at rates similar to the Ridgely loop (Table 2). Straightening, thus, appears not to have extended south of the mapped low-sinuosity floodplain. Much of the Bondurant strata are removed north of the preserved low-sinuosity reach and we cannot confidently determine if the straightening response extended into this area (Fig. 5A). We correlated conservatively and assumed that typical meandering prevailed here and straightening did not extend into this area. Reconstruction of the low-sinuosity channel was, thus, limited to the reach where strata of the low-sinuosity channel are preserved (Fig. 5). Strata of the low-sinuosity member are characterized by a complex succession of cutoff meander loops that obscured or eroded the initial channel remnants. The shape of the initial low-sinuosity channel is, thus, unknown, but minimum and maximum sinuosity estimates can still be made. The straightened channel of Fig. 5B represents the minimal-sinuosity channel possible within the confines of this floodplain, and the Reelfoot LS channel (Fig. 5A) would represent a reasonable maximum sinuosity attainable within this reach. The above channel estimates yield an approximate sinuosity drop from >2.5 to between 1.0 and 1.3 during this Bondurant straightening response.

Initiation for this straightening response is limited to somewhere within the interval between ~ 2200 BC and ~1600 BC and is more likely toward the early or middle part of this range (Fig. 6). Straightening must have begun after cutoff of the Hamby Pond loop soon after 2244 BC ±269, but was completed sometime before the oldest deposits dated within the low-sinuosity member (Needle Eye loop; 1620 BC±220) (Fig. 5 and 6; Table 1). Some of the low-sinuosity meandering predates the Needle Eye loop; however, reworking makes constraining the amount of this low-sinuosity meandering impractical.

The low-sinuosity meandering established during the middle-Holocene Bondurant straightening response continued for at least several hundred years and may have continued for up to ~1400 years. Middle-Holocene low-sinuosity meandering ended sometime after the youngest date recorded within the low-sinuosity member (Bondurant point bar, 1304 BC±306; Fig. 5). The Isom loop truncates the Bondurant low-sinuosity member and, thus, is younger. This low-sinuosity phase, therefore, must have ended before eventual abandonment of the Isom loop (798 BC+114/−69; Figs. 4 and 5). Maximum duration of low-sinuosity meandering is, thus, between 2244 BC±269 and 798 BC+35/−234, and minimum duration is between 1620 BC±220 and 1304 BC±306 (Fig. 6). Low-sinuosity meandering must have also maintained sufficient duration to accommodate growth of the succession of low-sinuosity meander loops preserved (Fig. 5A). At least 10 km of consecutive meandering is recorded within five sequential loops in the southern half of the low-sinuosity floodplain, and the time required to accrete these meanders represents a minimum duration for this low-sinuosity phase. Assuming a slow meander rate typical of the Ridgely meander, this would have required 1887 years. Even if the much faster short-term rates for localized maximum bar accretion (Hudson and Kesel, 2000; Table 2) were uncharacteristically maintained across the full length of each point bar for their full duration, this would still have required about 333 years. Probably most appropriate is the meander rate of the New Hubbard Lake loop, which similarly occupies a position within a low-sinuosity floodplain. At the rate of 7.6 m/yr that characterizes the New Hubbard Lake loop (Table 2), meandering within the Bondurant low-sinuosity member would have required about 1315 years.

A channel avulsion ended middle-Holocene low-sinuosity meandering as the Reelfoot LS channel was abandoned for a position farther west. Avulsion reinitiated meandering in an area that has since been reworked to form the New Madrid Alloformation (Fig. 5) and also positioned the meander axis from which the Tipptonville, Isom and, later, Hubbard Lake and Donaldson loops, would eventually derive (Fig. 4). This avulsion abandoned the Bondurant low-sinuosity floodplain for a position on the older Bondurant medium-sinuosity floodplain surface, which was 1.5 m higher in elevation.

4.2.2. Tectonic interpretation

The middle Holocene Bondurant record of river sinuosity is strikingly similar to that of the late Holocene New Madrid record and suggests an analogous history of fault control on river pattern. Medium-sinuosity meandering appears pervasive and no river response to faulting is evident in strata preserved within the Bondurant

medium-sinuosity member. The total duration of medium-sinuosity meandering is uncertain, but must have been confined to the interval between ~ 4292 BC and the ~2200 BC to ~1600 BC straightening response (Fig. 6), while still lasting the millennia needed to deposit this broad and well-developed meander belt (Fig. 5A). This is comparable to the period of >1700 years of uninterrupted meandering that is preserved in the New Madrid Alloformation and was coincident with Reelfoot fault quiescence preceding the ~AD 900 straightening response (Fig. 6). Middle Holocene straightening resulted in cutoff of at least three or four consecutive meander loops and a transition from a medium-sinuosity to a low-sinuosity channel in the reach directly upstream of the Reelfoot fault scarp. This straightening response did not induce meander cutoff and abrupt sinuosity drop down valley of the scarp where medium-sinuosity meandering continued and constructed the Ridgely and, later, Mooring loops (Fig. 5). The Bondurant straightening response (~2200 BC to ~1600 BC), like the later New Madrid straightening response (~AD 900), is interpreted to record local loss of channel gradient owing to Reelfoot fault slip and scarp uplift following a protracted tectonic quiescence (Fig. 6).

Notably, emerging liquefaction evidence argues for a high-magnitude seismic event originating from somewhere within the New Madrid seismic zone at 2350 BC+/− 200 years (Tuttle et al., 2005; Guccione, 2005). This is the only high-magnitude New Madrid earthquake event predating AD 300 identified so far from independent paleoseismic evidence, and is also the only event predating AD 900 that currently yields evidence for short-term temporal clustering of multiple high-magnitude earthquakes (Guccione, 2005). The timing of the ~2350 BC liquefaction event coincides with the initiation of Bondurant straightening (during the early part of the ~2200 BC to ~1600 BC interval, and starting as early as 2523 BC when measurement error considered). Liquefaction evidence does not identify the fault(s) sourcing these earthquakes. It seems reasonable to assert here, however, that at least one of the earthquakes within this ~2350 BC short-term cluster was caused by the same Reelfoot slip event which initiated Bondurant straightening.

The river avulsion that ended Bondurant deposition argues that at least one additional Reelfoot slip event occurred toward the end of low-sinuosity meandering, well after the event that initiated Bondurant straightening (Fig. 6). River avulsions commonly occur spontaneously on river floodplains because of processes intrinsic to fluvial systems and, thus, may occur without influence of forces external to the system, such as tectonics. Such intrinsic, or autocyclic, avulsions occur because the channel gradually builds an enveloping alluvial ridge that is higher than the adjacent floodplain. Channels will eventually aggrade sufficiently above the surrounding floodplain to prompt avulsion to an adjacent lower course without the influence of tectonics or other external factors (Slingerland and Smith, 1998; Jones and Schumm, 1999; Mohrig et al., 2000; Bridge, 2003). The abandoned Bondurant low-sinuosity surface, however, is 1.5 m lower than the adjacent medium-sinuosity surface onto which the river avulsed, and it is also 1.5 m lower than the New Madrid medium-sinuosity surface that was initiated by this avulsion. This is antithetical to the conditions required for an autocyclic avulsion and, thus, some external forcing mechanism is required to initiate avulsion. The most plausible explanation for this avulsion is that fault-induced uplift of the Reelfoot scarp blocked the river course that was then passing through the low-sinuosity floodplain (the Reelfoot LS Channel; Fig. 5A). This could have reduced channel gradients sufficiently in this reach to equalize the differences between slopes here and on the adjacent medium-sinuosity surface, facilitating avulsion (c.f. Holbrook and Schumm, 1999; Bridge, 2003).

Protracted meander suppression throughout deposition of the low-sinuosity member also argues for occurrence of additional slip in between the event that initiated straightening and the later event that caused avulsion (Fig. 6). The Mississippi River had leveled any remnant grade-controlling topography remaining on the Reelfoot scarp after Bondurant abandonment (after 1304 BC±306) and had returned to the characteristic meandering form of the medium-sinuosity New Madrid Allomember well before the New Madrid straightening response of AD 900. This suggests that low-sinuosity meandering will not maintain for millennial scales without continued sinuosity suppression by additional intermittent events. Despite several hundred to ~1400 years of successive meandering, the middle-Holocene low-sinuosity system never regained the higher sinuosity of precursory channels (Fig. 5), suggesting that the slopes needed to support the higher sinuosity of the prior and subsequent members did not exist during the time of low-sinuosity meandering. This extended period of low-sinuosity meandering is similar to the period following the AD 900 straightening response, wherein low slopes were maintained by two subsequent (AD 1450 and AD 1812) gradient-lowering slip episodes (Fig. 6). If the two slip events associated with straightening and avulsion that bracket the Bondurant low-sinuosity member were separated by the shorter estimate of several hundred years, low-sinuosity may potentially have been retained without the

force of an intermediate slip event. If these events were separated by the longer estimate of ~1400 years, however, at least one intermediate slip event is highly likely. Unlike river straightening and avulsion, meander suppression does not provide estimates for specific timing or number of driving fault-slip episodes. Lack of preserved middle-Holocene strata at the Reelfoot scarp also prevents further constraint of such individual recurrent uplift events.

4.3. Early-to-Middle Holocene Portageville Alloformation

4.3.1. Allostratigraphy

The Portageville Alloformation records all preserved river meandering prior to establishment of the Bondurant Alloformation. Channel-loop and point-bar allounits within the Portageville Alloformation are broadly similar in morphology to those of the New Madrid and Bondurant alloformations; however, this unit is not subdivided into allomembers. The oldest point bar dated in the Portageville Alloformation records deposition by a meandering Mississippi River by 5484 BC±367, and the youngest channel preserved in this unit was abandoned by 4292 BC+65/−245.

4.3.2. Interpretation

The floodplain segment preserved by the Portageville Alloformation does not straddle the Reelfoot fault and is small. As such, reliable inferences regarding early Holocene deformation on the Reelfoot fault cannot be made at this time from these strata. Of significance, however, the existence of the Portageville Alloformation does confirm that the Mississippi River existed as a meandering channel by this date. The river, thus, must have completed transition from its youngest braided glacial valley train (12,500–10,700 b.p., Blum et al., 2000; 12,500–12,100 b.p., Rittenour et al., 2003) to its current meandering form by 5484 BC±367 (Fig. 6).

5. Discussion

5.1. Evaluation of channel straightening as a paleoseismologic proxy

Channel straightening may be caused by factors other than fault-induced gradient reduction, namely climate-induced increase in stream and/or bed load discharge, lateral channel constriction by resistant strata, or autocyclic (system-intrinsic) meander-loop cutoff. The fault-induced gradient shift predicted by the AD 900 straightening response, however, is independently corroborated by other paleoseismic data from the New Madrid seismic zone. This directly supports a tectonic interpretation for this straightening response and, by analogy, indirectly supports a tectonic interpretation for the 2200–1600 BC straightening response. The following three observations provide additional support for a tectonic interpretation of these two straightening responses.

First, climate influences the lower Mississippi River by controlling the total water and sediment discharge delivered from upstream. Climate, however, has little ability to alter sinuosity-controlling variables over local river segments that lack major tributaries or major climatic boundaries. Furthermore, mapping of Holocene meander belts throughout the lower valley (Saucier, 1994) show no evidence of any regional climate-induced channel straightening comparable in time or degree to New Madrid and Bondurant straightening. Climatic variation would, thus, not well explain the localized sinuosity reduction characterized by these two straightening responses.

Second, lateral channel constriction has not had a major effect on channel morphology over the New Madrid and Bondurant straightened reaches. The modern river farther down valley does include local low-sinuosity reaches reflecting lateral channel constriction by locally impinging bedrock (Spitz and Schumm, 1997). Comparable bedrock constriction, however, is not characteristic of the more alluvial conditions which appear to have prevailed directly updip of the Reelfoot fault. Likewise, local bedrock control would not explain the observed temporal alternation between medium and low sinuosity observed in areas north of the Reelfoot fault.

Third, meander enlargement locally decreases the slope of the channel within an accreting meander loop without associated change in valley gradient. Continuation of this process will progressively lower stream power, which will eventually result in autocyclic loop cutoff and local channel straightening to reestablish channel gradient sufficient to transport available sediment load (Beerbower, 1964; Bridge, 2003). This process does not change external sinuosity-controlling variables of valley gradient or channel discharge or sediment load. Autocyclic straightening of an individual loop must, therefore, be compensated by increased sinuosity of adjacent loops, or else be extremely ephemeral. The two straightening responses described here cut off multiple consecutive meander loops with long-term maintenance of low sinuosity thereafter. This is atypical of autocyclic cutoff and highly suggestive of an enduring local change in valley gradient.

Even when non-tectonic causes are eliminated, channel straightening still has interpretive limitations as a tectonic proxy. Particularly, straightening will only record slip episodes that generate a vertical component of surficial

displacement. This uplift must also obstruct the channel course and alter channel gradient sufficiently to induce a tectonic response. For instance, the New Madrid strike-slip faults are kinematically coupled with the Reelfoot fault (Fig. 1) and likely experienced displacement with each major Reelfoot slip event (Russ, 1982; Johnston and Schweig, 1996; Van Arsdale et al., 1998). These strike-slip faults generate mostly lateral displacement, which does not alter valley or channel gradient and, thus, causes no definitive shifts in sinuosity across multiple loops. Further, secondary Holocene uplift mapped above these strike-slip faults (i.e., the Ridgely Ridge; Russ, 1982; Johnston and Schweig, 1996; Van Arsdale et al., 1998) is oriented subparallel with the channel and would be unlikely to cause more than a minor channel deflection. Slip on these faults was not detected by our technique. In contrast, Reelfoot fault displacement sufficient to substantially deform the floodplain surface will be detectable because this deformation will manifest as uplift (Russ, 1982; Kelson et al., 1996) and because all Holocene river courses crossed the fault trace (Figs. 1 and 3). Numerous historic earthquakes with magnitudes less than the AD 1812 event are attributed to the Reelfoot fault (Fig. 1), but these produce no noticeable surface deformation (Russ, 1982; Kelson et al., 1996). Therefore our technique detects only deformation related to Reelfoot slip events of AD 1812 scale.

Straightening responses are most suited to resolve slip episodes that follow a period of quiescence sufficiently long to permit the river to bevel any tectonic features causing gradient perturbation and return to a regionally consistent meandering form. Slip events following any sooner after an initial episode of tectonic river straightening will prolong the lowered sinuosity caused by the earlier event, but these events will be difficult to resolve individually by assessing sinuosity effects. For instance, the second (AD 1450) and third (AD 1812) slip events that followed the AD 900 straightening response are known because of paleoseismic and historic data. Although they sustained straightening and forced additional gradient responses, they occurred in too rapid a succession after the AD 900 event to be easily resolved by ascertaining meander cutoff.

5.2. Implications for seismic trends in the New Madrid seismic zone and surrounding U.S. Mid-Continent

Paleoseismic data from prior and independent studies record that slip on the Reelfoot fault triggered three earthquake episodes over the past 1100 years, and that this seismically active period was preceded by at least 1700 years of relative quiescence (Russ, 1982; Kelson et al., 1996; Guccione et al., 2002; Tuttle et al., 2002). Sinuosity patterns of the late-Holocene Mississippi River record this as a period of meandering during initial tectonic quiescence, followed by a straightening response abruptly after the first slip episode (~AD 900), and followed in turn by continued suppression of sinuosity through subsequent slip episodes (Fig. 6). The preceding middle-Holocene record of sinuosity is analogous. Middle-Holocene channels reveal an enduring tectonic quiescence that ended with a period of several hundred to ~1400 years of tectonic channel straightening (beginning between ~2200 BC and ~1600 BC), which was caused by Reelfoot fault slip (Fig. 6). This middle-Holocene episode of low sinuosity apparently ended with a fault-induced river avulsion and was likely maintained by one or more intermittent slip events. These observations argue that two or more discrete slip events occurred on the Reelfoot fault during middle-to-late-Holocene deposition of the Bondurant low-sinuosity member. These occurred prior to the late-Holocene New Madrid slip events that are currently known and constitute newly proposed Reelfoot fault-slip events.

These Bondurant events are interspersed comparably to the three latter New Madrid slip events, but are collectively separated from the first of these latter New Madrid events by a longer duration without notable fault displacement (Fig. 6). Particularly, Reelfoot fault slip occurs during a previously undocumented middle-to-late-Holocene cluster of two or more events with century-scale spacing, which is separated from the well-known late-Holocene seismic episode by at least 1700 years of tectonic quiescence. This suggests that major slip on the Reelfoot fault was temporally clustered on millennial scales.

Interpretation of millennial-scale temporal clustering on the New Madrid system has implications for future assessment of slip trends on U.S. Mid-continent faults near the New Madrid seismic zone. Several faults and fault zones within 200 km of the Reelfoot fault have weak to moderate modern seismicity, yet paleoseismic evidence is found there for significant large earthquakes earlier in the Holocene. These faults are summarized in Wheeler and Crone (2001) and include the Commerce lineament (Harrison and Schultz, 1994); the Wabash Valley fault zone (Obermeier et al., 1991); and the southern Reelfoot rift margin (Cox et al., 2001) (Fig. 1). Deformation trends on these faults are poorly known, and the potential for reactivation makes them a concern for future seismic hazard in the U.S. Mid-continent (Wheeler and Crone, 2001). If these faults slip in temporal clusters similarly to the pattern proposed here for the New Madrid system, the possibility then exists that some or all of these faults are presently within their dormant phase. Moreover, some models for millennial-

scale temporal clustering imply fault interaction as the driving mechanism (Peltzer et al., 2001; Chery et al., 2001). The possibility that activity could alternate between the Reelfoot fault and one or more of these other fault systems is, thus, a reasonable hypothesis as well. In fact, it has already been proposed that strain on the southern strike-slip fault of the current New Madrid system is in the process of slowly shifting to the southern Reelfoot rift margin (Cox et al., 2001).

5.3. Implications for intrapalte faulting and mid-continent seismic hazard

Millennial-scale temporal clustering of co-seismic fault slip is not previously documented from the slowly deforming compressive stress provinces typical of deep continental interiors. The potential for such clustering, however, has long been implicit from mid-continent deformation models (e.g., Talwani, 1988; Marshak and Paulsen, 1996). Recent works have further speculated that millennial-scale clustering is likely in compressive continental interiors, based on observations of similar fault behavior in more rapidly deforming continental regions directly affiliated with active plate margins (Peltzer et al., 2001; Chery et al., 2001). Our study of the New Madrid seismic zone supports these prior assertions by offering a proxy record of millennial-scale temporal clustering of slip events from an active mid-continent intraplate fault.

This concept of temporal clustering carries additional ramifications for mid-continent faulting relevant to future studies of continental interiors. Long-term clustering implies that midplate faults lacking evidence for intensive near-historic seismicity can unexpectedly and abruptly become serious seismic hazards in the future, and faults presently posing a seismic hazard can become dormant. Crone et al. (2003) recently stressed this point. They found evidence for periods of quiescence lasting 10^4–10^5 years on mid-continent faults in Australia and argue that reactivation of mid-continent faults with no prior warning could be the norm. For instance, the catastrophic 2001 Bhuj earthquake (M_w 7.6) in northern India appears to have occurred on a thrust fault in a compressive plate interior with many tectonic similarities, though not necessarily identical (Stein et al., 2001), to the New Madrid system (Schweig et al., 2003; Bodin and Horton, 2004). No prior record of major seismicity was known on this thrust fault before this large event (Bodin and Horton, 2004).

Results of this study also imply a potential hierarchical nature to earthquake clustering on the Reelfoot and contiguous New Madrid fault system. If the short-term monthly to yearly temporal clusters characteristic of late-Holocene (AD 900 and younger) earthquake episodes are representative of the middle-Holocene events as well, then short-term clusters are themselves elements of longer-term millennial clusters. Emerging liquefaction evidence for a short-term temporally clustered seismic event at 2350 BC +/− 200 years (Tuttle et al., 2005; Guccione, 2005) near the initiation of the middle-Holocene Bondurant millennial cluster argues that this indeed could be the case. Similarly, short-term clusters are elements of millennial-scale clusters if the late-Holocene earthquakes are actually part of an uncompleted New-Madrid millennial cluster. In addition, the cumulative deformation recorded on the New Madrid fault system is likely young (Schweig and Ellis, 1994) and may have begun as recently as the beginning of the Holocene (Van Arsdale, 2000; Grollimund and Zoback, 2001). Cretaceous to modern deformation trends on the Reelfoot fault and larger New Madrid system suggest that Holocene-scale deformation occurs in short bursts of 10^4 years, with longer quiescent periods of as much as 10^6 years in between (Van Arsdale, 2000). The Holocene set of millennial-scale clusters could, thus, record a burst of activity within some longer-term fault cycle. Applied generally, the occurrence of monthly-scaled clustering within millennial-scale clustering, potentially within longer-scale clustering of Reelfoot fault slip, would infer that temporal clustering is hierarchical on some mid-continent faults.

6. Conclusions

1) Evaluation of tectonic effects on channels reconstructed from Mississippi River Holocene strata reaffirm previous assertions for an episode of recent seismicity on the high-hazard Reelfoot fault beginning near AD 900, and provide additional evidence for at least two previously undocumented fault slip events earlier during the Holocene (~2200 BC to ~1600 BC and ~1304 BC to ~798 BC, respectively). The probability for an additional event(s) between these two pre-AD 900 events is enhanced as the time estimate between the two is increased.
2) This study constrains tectonic response times for channel pattern change in large alluvial rivers. Destructive river-pattern responses like channel straightening can reorder channels substantially on time scales of $\leq 3 \times 10^2$ yr, and thus provide good indicators for vertical fault slip events separated by time intervals sufficient to permit channel recovery. Channel recovery time is determined by the time needed to bevel gradient-altering tectonic topography and to construct new bar complexes, and is ~1000 yr for the

Mississippi River in the New Madrid seismic zone. Constructive pattern responses like sinuosity increase are limited by the rate of growth for bar complexes and may require several centuries to complete. They are thus generally less time sensitive tectonic proxies than destructive pattern responses and are also more challenging to physically and temporally constrain.

3) This study provides the first direct evidence for millennial-scale temporal clustering of large slip events on a fault in a compressive mid-continent intraplate region. These data make a first case for a ~1000 year cluster of earthquakes with 10^2 yr spacing on the Reelfoot fault, beginning with a co-seismic slip event near the end of the middle-Holocene at ~2200 BC to ~1600 BC. This Holocene cluster appears separated from the modern episode of seismicity (beginning ~AD 900) by at least 1700 years of tectonic quiescence.
4) Millennial-scale temporal clustering of slip events infers that faults can reactivate and deactivate over millennial time periods. The potential for historically quiescent faults to suddenly become hazardous and the potential of currently hazardous faults to become quiescent over millennial scales should, thus, be considered in seismic hazard models for continental interiors.
5) The Reelfoot fault reveals evidence for temporal clustering of slip events on monthly scales, millennial scales, and potentially on scales of 10^4–10^6 years. The potential does exist, therefore, that temporal clustering can be hierarchical for at least some mid-continent faults.
6) Stratigraphic proxy data, such as that used in this study, can reveal information regarding trends in fault displacement that are not resolved by more utilized methods. Stratigraphic approaches may thus have underutilized potential as a paleoseismic tool.

Acknowledgments

We gratefully acknowledge support by the donors of The Petroleum Research Fund, administered by the American Chemical Society. Southeast Missouri State University provided additional funding, and NASA donated satellite imagery. Alan Bornstien taxonomically identified all plant material prior to radiocarbon dating. Thanks to Eugene Schweig, Martitia Tuttle, Roy Van Arsdale, Mike Blum, Peggy Guccione, Pradeep Talwani and five additional anonymous reviewers for valuable input during development of this paper. Thanks also go to Ronald Van Balen and Karl Mueller for review and valuable input into the current version of this paper. High credit also goes to student colleagues: Craig Cox, Susan Kirkwood, Clayton Sneed, and Eric Stevenson.

Appendix A. Supplementary data

Supplementary data associated with this article can be found, in the online version, at doi:10.1016/j.tecto.2006.04.002.

References

Aslan, A., Autin, W.J., 1998. Holocene floodplain soil formation in the southern lower Mississippi Valley: implications for interpreting alluvial paleosols. Geological Society of America Bulletin 110, 433–449.

Autin, W.J., 1992. Use of alloformations for definition of Holocene meander belts in the middle Amite River, southern Louisiana. Geological Society of America Bulletin 104, 233–241.

Bakun, W.H., Hopper, M.G., 2004. Magnitudes and locations of the 1811–1812 New Madrid, Missouri, and the 1886 Charleston, South Carolina, earthquakes. Bulletin of the Seismological Society of America 94 (1), 64–75.

Beerbower, J.R., 1964. Cyclothems and cyclic depositional mechanisms in alluvial plain sedimentation. Geological Survey of Kansas Bulletin 169, 31–42.

Blum, M.D., Guccione, M.J., Wysocki, D.A., Robnett, P.C., Ruttledge, M., 2000. Late Pleistocene evolution of the lower Mississippi Valley, Southern Missouri to Arkansas. Geological Society of America Bulletin 112, 221–235.

Bodin, P., Horton, S., 2004. Source parameters and tectonic implications of aftershocks of the *M* (sub w) 7.6 Bhuj earthquake of 26 January 2001. Bulletin of the Seismological Society of America 94 (3), 818–827.

Boyd, K.F., Schumm, S.A., 1995. Geomorphic evidence of deformation in the northern part of the New Madrid seismic zone. U.S.G.S. Professional Paper, vol. 1538-R, p. 35.

Bridge, J.S., 2003. Rivers and Floodplains; Forms, Processes, and Sedimentary Record. Blackwell Publishing, Oxford, UK, p. 491.

Champion, J., Mueller, K., Tate, A., Guccione, M., 2001. Geometry, numerical models, and revised slip rate for the Reelfoot fault trishear fault-propagation fold, New Madrid seismic zone. Engineering Geology 62, 31–49.

Chery, J., Merkel, S., Bouissou, S., 2001. A physical basis for time clustering of large earthquakes. Bulletin of the Seismological Society of America 91 (6), 1685–1693.

Clark, D., Leonard, M., 2003. Principal stress orientation from multiple focal-plane solutions; new insights into the Australian intraplate stress field. In: Hills, R.R., Mueller, R.D. (Eds.), Evolution and Dynamics of the Australian Plate Geological Society of America Special Paper, vol. 372, pp. 91–105.

Cox, R.T., Van Arsdale, R.B., Harris, J.B., Larson, D., 2001. Neotectonics of the southeastern Reelfoot rift margin, central United States, and implications for regional strain accommodation. Geology 29 (5), 419–422.

Cramer, C.H., Wheeler, R.L., Frankel, A.D., Talwani, P., Lee, R.C., 2001. Incorporating uncertainty into probablistic seismic hazard maps for the central and eastern U.S. Seismological Research Letters 72, 127.

Crone, A.J., de Martini, P.M., Machette, M.N., Okumura, K., Presscott, J.R., 2003. Paleoseismicity of two historically quiescent faults in Australia; implications for fault behavior in stable continental regions. Bulletin of the Seismological Society of America 93 (5), 1913–1934.

Grollimund, B., Zoback, M.D., 2001. Did deglaciation trigger intraplate seismicity in the New Madrid seismic zone? Geology 29 (2), 175–178.

Guccione, M.J., 2005. Late Pleistocene and Holocene paleoseismology of an intraplate seismic zone in a large alluvial valley, the New Madrid seismic zone, central USA. Tectonophysics 408, 237–264.

Guccione, M.J., Mueller, K., Champion, J., Shepard, S., Carlson, S.D., Odhiambo, B., Tate, A., 2002. Stream response to repeated coseismic folding, Tiptonville dome, New Madrid seismic zone. Geomorphology 43, 313–349.

Harrison, R.W., Schultz, A., 1994. Strike-slip faulting at Thebes Gap, Missouri — implications for New Madrid tectonism. Tectonics 13, 246–257.

Holbrook, J.M., Schumm, S.A., 1999. Geomorphic and sedimentary response of rivers to tectonic deformation: a brief review and critique of a tool for recognizing subtle epeirogenic deformation in modern and ancient settings. Tectonophysics 305, 287–306.

Holbrook, J.M., Autin, W., Rittenour, T.M., Marshak, S., 2002. A Mississippi River Record of Millennial-Scale Punctuated Displacement in the New Madrid Seismic Zone; Implications for Apparently Placid Faults. GSA Annual Meeting, Denver, Colorado.

Hough, G., Armbruster, J.G., Seeber, L., Hough, J.F., 2000. On the modified Mercalli intensities and magnitudes of the 1811–1812 New Madrid, central U.S. earthquakes. Journal of Geophysical Research 100, 23,839–23,864.

Hudson, P.F., Kesel, R.H., 2000. Channel migration and meander-bend curvature in the lower Mississippi River prior to major human modification. Geology 28 (6), 531–534.

Johnston, A.C., Schweig, E.S., 1996. The enigma of the New Madrid earthquakes of 1811–1812. Annual Review of Earth and Planetary Sciences 24, 339–384.

Jones, L.S., Schumm, S.A., 1999. Causes of avulsion: an overview. In: Smith, N.D., Rogers, J. (Eds.), Fluvial Sedimentology VI International Association of Sedimentologists Special Publication, vol. 28, pp. 171–178.

Kelson, K., Simpson, G.D., Van Arsdale, R.B., Haraden, C.C., Lettis, W.R., 1996. Multiple late Holocene earthquakes along the Reelfoot fault, central New Madrid seismic zone. Journal of Geophysical Research 101 (B3), 6151–6170.

Kenner, S.J., Segall, P., 2000. A mechanical model for intraplate earthquakes: application to the New Madrid seismic zone. Science 289, 2329–2332.

Marshak, S., Paulsen, T., 1996. Midcontinent U. S. faults and fault zones: a legacy of Proterozoic intracratonic extensional tectonism. Geology 24, 151–154.

Mittag, R.J., 2003. Fractal analysis of earthquake swarms of Vogtland/NW-Bohemia intraplate seismicity. Journal of Geodynamics 35 (1–2), 173–189.

Mohrig, D., Heller, P.L., Paola, C., Lyons, W.J., 2000. Interpreting avulsion process from ancient alluvial sequences: Guadolope–Matarranya system (northwestern Spain) and Wasatch Formation (western Colorado). Bulletin of the Geological Society of America 112, 1787–1803.

Mueller, K., Pujol, J., 2001. Three-dimensional geometry of the Reelfoot blind thrust: implications for moment release and earthquake magnitude in the New Madrid seismic zone. Bulletin of the Seismological Society of America 91 (6), 1563–1573.

Mueller, K., Champion, J., Guccione, M., Kelson, K., 1999. Fault slip rates in the modern New Madrid seismic zone. Science 286, 1135–1138.

Newman, A., Schneider, J., Stein, S., Mendex, A., 2001. Uncertainties in seismic hazard maps for the New Madrid seismic zone and implications for seismic hazard communication. Seismological Research Letters 72, 647–663.

Obermeier, S.F., Bleuer, N.R., Munson, C.A., Munson, P.J., Martin, W.S., McWilliams, K.M., Tabaczynski, D.A., Odum, J.K., Rubin, M., Eggert, D.L., 1991. Evidence of strong earthquake shaking in the lower Wabash Valley from prehistoric liquefaction features. Science 251, 1061–1063.

Ouchi, S., 1985. Response of alluvial rivers to slow active tectonic movement. Geological Society of America Bulletin 96, 504–515.

Odum, J.K., Stephenson, W.J., Shedlock, K.M., Pratt, T.L., 1998. Near-surface structural model for deformation associated with the February 7, 1812, New Madrid, Missouri earthquake. Geological Society of America Bulletin 110, 149–162.

Peltzer, G., Crampe, F., Hensley, S., Rosen, P., 2001. Transient strain accumulation and fault interaction in the eastern California shear zone. Geology 29, 975–978.

Purser, J.L., Van Arsdale, R.B., 1998. Structure of the Lake County uplift, New Madrid seismic zone. Bulletin of the Seismological Society of America 88, 1204–1211.

Reimer, P.J., Baillie, M.G.L., Bard, E., Bayliss, A., Beck, J.W., Bertrand, C.J.H., Blackwell, P.G., Buck, C.E., Burr, G.S., Cutler, K.B., Damon, P.E., Edward, R.L., Fairbanks, R.G., Friedrich, M., Guilderson, T.P., Hogg, A.G., Hughen, K.A., Kromer, B., McCormac, F.G., Manning, S.W., Ramsey, C.B., Reimer, R.W., Remmele, S., Southon, J.R., Stuiver, M., Talamo, S., Taylor, F.W., van der Plicht, J., Weyhenmeyer, C.E., 2004. IntCal04 Terrestrial radiocarbon age calibration, 26 – 0 ka BP. Radiocarbon 46, 1029–1058.

Rittenour, T.M., Goble, R.J., Blum, M.D., 2003. An optical age chronology of Late Pleistocene fluvial deposits in the northern lower Mississippi Valley. Quaternary Science Reviews 22, 1105–1110.

Russ, D.P., 1982. Style and significance of surface deformation in the vicinity of New Madrid, Missouri. In: McKeown, F.A., Pakiser, L.C. (Eds.), Investigations of the New Madrid, Missouri, Earthquake Region U. S. G. S. Professional Paper, vol. 1236, pp. 95–114.

Saucier, R.T., 1994. Geomorphology and Quaternary Geologic History of the Lower Mississippi Valley. U. S. Army Corps of Engineers, Mississippi River Commission, Vicksburg, Mississippi, p. 364.

Schulte, S., Mooney, W.D., 2003. Earthquakes in continental interiors; a global study. Geological Society of America Annual Meeting Abstracts with Programs, vol. 35 (6), p. 152.

Schumm, S.A., Dumont, J.F., Holbrook, J.M., 2000. Active Tectonics and Alluvial Rivers. Cambridge University Press, Cambridge, UK, p. 276.

Schweig, E.S., Ellis, M.A., 1994. Reconciling short recurrence intervals with minor deformation in the New Madrid seismic zone. Science 264, 1308–1311.

Schweig, E., Gombert, J., Petersen, M., Ellis, M., Bodin, P., Mayrose, L., Rastogi, B.K., 2003. The M_w 7.7 Bhuj earthquake; global lessons for earthquake hazard in intra-plate regions. Journal of the Geological Society of India 61 (3), 277–282.

Slingerland, R.L., Smith, N.D., 1998. Necessary conditions for a meandering-river avulsion. Geology 26, 435–438.

Spicak, A., 2000. Earthquake swarms and accompanying phenomena in intraplate regions: a review. Studia Geophysica et Geodaetica 44, 89–106.

Spitz, W.J., Schumm, S.A., 1997. Tectonic geomorphology of the Mississippi Valley between Osceola, Arkansas and Friar's Point, Mississippi. Engineering Geology 46, 259–280.

Stein, S., Schoonover, M., Sella, G.F., Okal, E., 2001. Bhuj; a diffuse plate boundary zone earthquake? Geological Society of America Annual Meeting Abstracts with Program, vol. 33 (6), p. 396.

Talwani, P., 1988. The intersection model for intraplate earthquakes. Seismological Research Letters 59, 305–310.

Tornqvist, T.E., Van Dijk, G.J., 1993. Optimizing sampling strategy for radiocarbon dating of Holocene fluvial systems in a vertically aggrading setting. Boreas 22, 129–145.

Tuttle, M.P., Collier, J., Wolf, L.W., Lafferty III, R.H., 1999. New evidence for a large earthquake in the New Madrid seismic zone between A.D. 1400 and 1670. Geology 27, 771–774.

Tuttle, M.P., Schweig, E.S., Sims, J.D., Lafferty, R.H., Wolf, L.W., Haynes, M.L., 2002. The earthquake potential of the New Madrid seismic zone. Bulletin of the Seismological Society of America 92 (6), 2080–2089.

Tuttle, M.P., Schweig III, E.S., Campbell, J., Thomas, P.M., Sims, J.D., Lafferty III, R.H., 2005. Evidence for New Madrid earthquakes in A.D. 300 and 2350 B.C. Seismological Research Letters 76, 489–501.

Van Arsdale, R.B., 2000. Displacement history and slip rate on the Reelfoot fault of the New Madrid seismic zone. Engineering Geology 55, 219–226.

Van Arsdale, R.B., Purser, J., Stephenson, W., Odum, J., 1998. Faulting along the southern margin of Reelfoot Lake, Tennessee. Bulletin of the Seismological Society of America 88, 131–139.

Wheeler, R.L., Crone, A.J., 2001. Known and suggested quaternary faulting in the Mid-continent United States. Engineering Geology 62, 51–78.

Zoback, M.L., Mooney, W.D., 2003. Lithospheric buoyancy and continental intraplate stress. International Geology Review 45 (2), 95–118.

Zoback, M.L., Zoback, M., 1980. State of stress in the conterminous United States. Journal of Geophysical Research 85 (B11), 6113–6156.

Zoback, M.L., et al., 1989. Global patterns of tectonic stress. Nature 341, 291–298.